

The inverse problem in hadron structure from lattice QCD

Martha Constantinou



Temple University

**Tackling The Real-Time Challenge In Strongly Correlated Systems:
Spectral Properties From Euclidean Path Integrals**

September 13 - 17, 2021

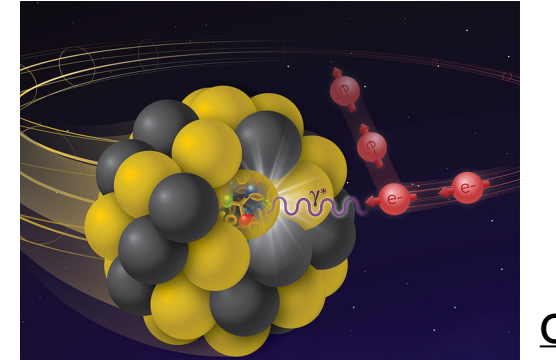
OUTLINE

- ★ Formulation of the problem
- ★ Limitations of lattice data in accessing x-dependent PDFs (quasi-PDFs method)
- ★ Other reconstruction methods (Backus Gilbert)
- ★ Alternative methods to quasi-PDFs (pseudo-PDFs)
- ★ Naive vs advanced reconstruction methods (FT, BG, fitting reconstruction)
- ★ Concluding remarks

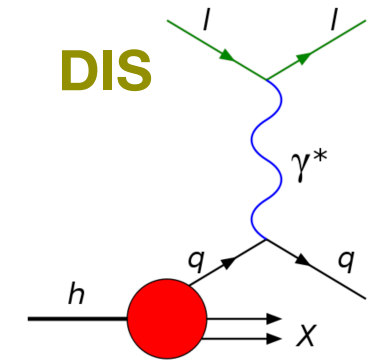
The problem: PDF reconstruction from lattice data

Hadron Structure

- ★ Structure of hadrons explored in high-energy scattering processes



Collisions @ EIC

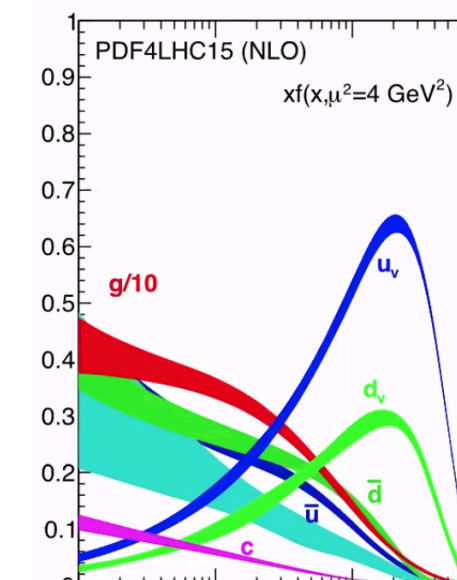


- ★ Processes cross-section contains information on hadron

$$\sigma_{\text{DIS}}(x, Q^2) = \sum_i [H_{\text{DIS}}^i \otimes f_i](x, Q^2)$$

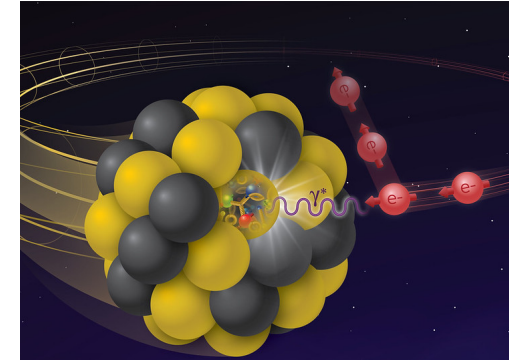
$$[a \otimes b](x) \equiv \int_x^1 \frac{d\xi}{\xi} a\left(\frac{x}{\xi}\right) b(\xi)$$

- ★ Hadron structure expressed in terms of distribution functions of partonic constituents (PDFs, GPDs, TMDs)
- ★ In hard scattering processes the partons propagate along the light-cone.

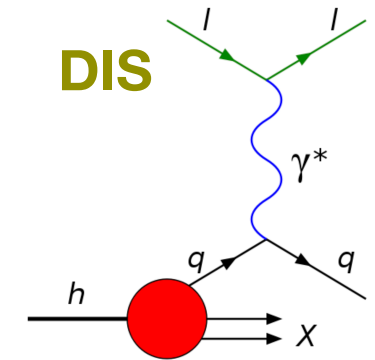


Hadron Structure

- ★ Structure of hadrons explored in high-energy scattering processes



Collisions @ EIC



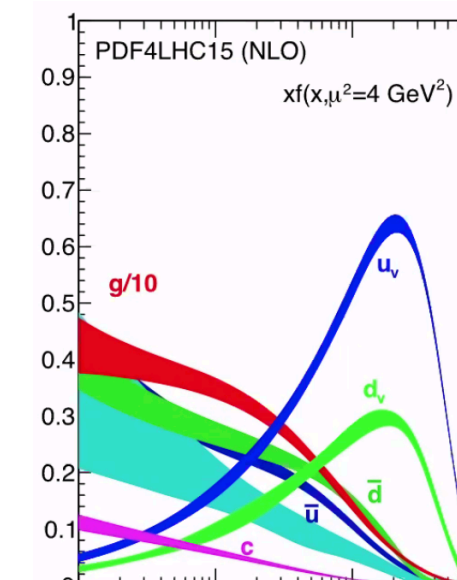
- ★ Processes cross-section contains information on hadron

$$\sigma_{\text{DIS}}(x, Q^2) = \sum_i [H_{\text{DIS}}^i \otimes f_i](x, Q^2)$$

$$[a \otimes b](x) \equiv \int_x^1 \frac{d\xi}{\xi} a\left(\frac{x}{\xi}\right) b(\xi)$$

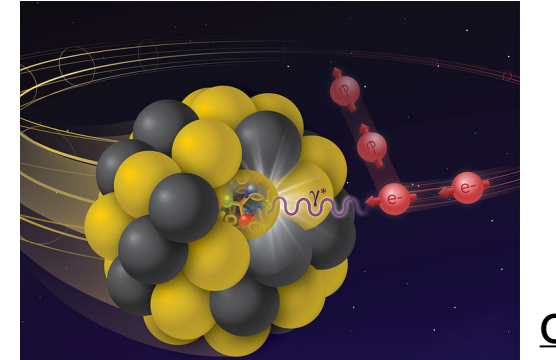
Perturb. part
(process dependent)

- ★ Hadron structure expressed in terms of distribution functions of partonic constituents (PDFs, GPDs, TMDs)
- ★ In hard scattering processes the partons propagate along the light-cone.

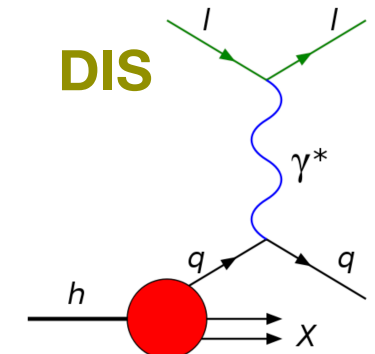


Hadron Structure

- ★ Structure of hadrons explored in high-energy scattering processes



Collisions @ EIC



- ★ Processes cross-section contains information on hadron

$$\sigma_{\text{DIS}}(x, Q^2) = \sum_i [H_{\text{DIS}}^i \otimes f_i](x, Q^2)$$

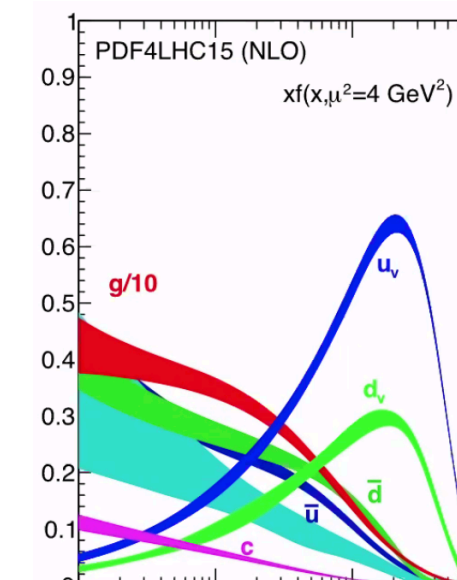
$$[a \otimes b](x) \equiv \int_x^1 \frac{d\xi}{\xi} a\left(\frac{x}{\xi}\right) b(\xi)$$

Perturb. part
(process dependent)

Non-Perturb. part
(process “independent”)

- ★ Hadron structure expressed in terms of distribution functions of partonic constituents (PDFs, GPDs, TMDs)

- ★ In hard scattering processes the partons propagate along the light-cone.



Distribution Functions

- ★ In parton model, the physical picture is valid for the infinite momentum frame.
- ★ DFs parameterized in terms of off-forward matrix elements of non-local light-cone operators

[R. P. Feynman, Phys. Rev. Lett. 23, 1415 (1969)]

$$f(x) = \frac{1}{4\pi} \int dy^- e^{-ixP^+y^-} \langle P, S | \bar{\psi}_f \gamma^+ \mathcal{W} \psi_f | P, S \rangle \quad y^\pm = \frac{1}{2}(y^0 \pm y^3)$$

Distribution Functions

- ★ In parton model, the physical picture is valid for the infinite momentum frame.

- ★ DFs parameterized in terms of off-forward matrix elements of non-local light-cone operators

[R. P. Feynman, Phys. Rev. Lett. 23, 1415 (1969)]

$$f(x) = \frac{1}{4\pi} \int dy^- e^{-ixP^+y^-} \langle P, S | \bar{\psi}_f \gamma^+ \mathcal{W} \psi_f | P, S \rangle \quad y^\pm = \frac{1}{2}(y^0 \pm y^3)$$

- ★ DFs are not accessible on a Euclidean lattice. Instead one calculates an object with the fields spatially separated

[X. Ji, Phys. Rev. Lett. 110 (2013) 262002]

$$\tilde{q}_\Gamma(x, t, \xi, P_3, \mu) = \int_{-\infty}^{\infty} \frac{dz}{4\pi} e^{-ixP_3z} \langle N(P_f) | \bar{\Psi}(z) \Gamma \mathcal{W}(z, 0) \Psi(0) | N(P_i) \rangle_\mu$$

Distribution Functions

- ★ In parton model, the physical picture is valid for the infinite momentum frame.
- ★ DFs parameterized in terms of off-forward matrix elements of non-local light-cone operators [R. P. Feynman, Phys. Rev. Lett. 23, 1415 (1969)]

$$f(x) = \frac{1}{4\pi} \int dy^- e^{-ixP^+y^-} \langle P, S | \bar{\psi}_f \gamma^+ \mathcal{W} \psi_f | P, S \rangle \quad y^\pm = \frac{1}{2}(y^0 \pm y^3)$$

- ★ DFs are not accessible on a Euclidean lattice. Instead one calculates an object with the fields spatially separated [X. Ji, Phys. Rev. Lett. 110 (2013) 262002]

$$\tilde{q}_\Gamma(x, t, \xi, P_3, \mu) = \int_{-\infty}^{\infty} \frac{dz}{4\pi} e^{-ixP_3z} \underbrace{\langle N(P_f) | \bar{\Psi}(z) \Gamma \mathcal{W}(z, 0) \Psi(0) | N(P_i) \rangle_\mu}_{\downarrow}$$

Core ingredient of
lattice calculation

Distribution Functions

- ★ In parton model, the physical picture is valid for the infinite momentum frame.
- ★ DFs parameterized in terms of off-forward matrix elements of non-local light-cone operators [R. P. Feynman, Phys. Rev. Lett. 23, 1415 (1969)]

$$f(x) = \frac{1}{4\pi} \int dy^- e^{-ixP^+y^-} \langle P, S | \bar{\psi}_f \gamma^+ \mathcal{W} \psi_f | P, S \rangle \quad y^\pm = \frac{1}{2}(y^0 \pm y^3)$$

- ★ DFs are not accessible on a Euclidean lattice. Instead one calculates an object with the fields spatially separated [X. Ji, Phys. Rev. Lett. 110 (2013) 262002]

$$\tilde{q}_\Gamma(x, t, \xi, P_3, \mu) = \int_{-\infty}^{\infty} \frac{dz}{4\pi} e^{-ixP_3z} \frac{\langle N(P_f) | \bar{\Psi}(z) \Gamma \mathcal{W}(z, 0) \Psi(0) | N(P_i) \rangle_\mu}{\downarrow \text{Quasi-distribution} \quad \downarrow \text{Core ingredient of lattice calculation}}$$

Distribution Functions

- ★ In parton model, the physical picture is valid for the infinite momentum frame.
 - ★ DFs parameterized in terms of off-forward matrix elements of non-local light-cone operators

$$f(x) = \frac{1}{4\pi} \int dy^- e^{-ixP^+y^-} \langle P, S | \bar{\psi}_f \gamma^+ \mathcal{W} \psi_f | P, S \rangle \quad y^\pm = \frac{1}{2}(y^0 \pm y^3)$$

- ★ DFs are not accessible on a Euclidean lattice. Instead one calculates an object with the fields spatially separated [X. Ji, Phys. Rev. Lett. 110 (2013) 262002]

$$\tilde{q}_\Gamma(x, t, \xi, P_3, \mu) = \int_{-\infty}^{\infty} \frac{dz}{4\pi} e^{-i x P_3 z} \langle N(P_f) | \bar{\Psi}(z) \Gamma \mathcal{W}(z, 0) \Psi(0) | N(P_i) \rangle_\mu$$

Quasi-distribution Manifestation of
INVERSE PROBLEM Core ingredient of
lattice calculation

Distribution Functions

★ Alternative approaches proposed, e.g.:

Hadronic tensor

[K.F. Liu, S.J. Dong, PRL 72 (1994) 1790, K.F. Liu, PoS(LATTICE 2015) 115]

Auxiliary scalar quark

[U. Aglietti et al., Phys. Lett. B441, 371 (1998), arXiv:hep-ph/9806277]

Fictitious heavy quark

[W. Detmold, C. J. D. Lin, Phys. Rev. D73, 014501 (2006)]

Auxiliary scalar quark

[V. Braun & D. Mueller, Eur. Phys. J. C55, 349 (2008), arXiv:0709.1348]

Higher moments

[Z. Davoudi, M. Savage, Phys. Rev. D86, 054505 (2012)]

Quasi-distributions (LaMET)

[X. Ji, PRL 110 (2013) 262002, arXiv:1305.1539; Sci. China PPMA. 57, 1407 (2014)]

Compton amplitude and OPE

[A. Chambers et al. (QCDSF), PRL 118, 242001 (2017), arXiv:1703.01153]

Pseudo-distributions

[A. Radyushkin, Phys. Rev. D 96, 034025 (2017), arXiv:1705.01488]

Good lattice cross sections

[Y-Q Ma & J. Qiu, Phys. Rev. Lett. 120, 022003 (2018), arXiv:1709.03018]

Distribution Functions

★ Alternative approaches proposed, e.g.:

Hadronic tensor

[K.F. Liu, S.J. Dong, PRL 72 (1994) 1790, K.F. Liu, PoS(LATTICE 2015) 115]

Auxiliary scalar quark

[U. Aglietti et al., Phys. Lett. B441, 371 (1998), arXiv:hep-ph/9806277]

Fictitious heavy quark

[W. Detmold, C. J. D. Lin, Phys. Rev. D73, 014501 (2006)]

Auxiliary scalar quark

[V. Braun & D. Mueller, Eur. Phys. J. C55, 349 (2008), arXiv:0709.1348]

Higher moments

[Z. Davoudi, M. Savage, Phys. Rev. D86, 054505 (2012)]

Quasi-distributions (LaMET)

[X. Ji, PRL 110 (2013) 262002, arXiv:1305.1539; Sci. China PPMA. 57, 1407 (2014)]

Compton amplitude and OPE

[A. Chambers et al. (QCDSF), PRL 118, 242001 (2017), arXiv:1703.01153]

Pseudo-distributions

[A. Radyushkin, Phys. Rev. D 96, 034025 (2017), arXiv:1705.01488]

Good lattice cross sections

[Y-Q Ma & J. Qiu, Phys. Rev. Lett. 120, 022003 (2018), arXiv:1709.03018]

See talks by:

- Kostas Orginos (Wednesday)
- Keh-Fei Liu (Friday)

Limitations of lattice data

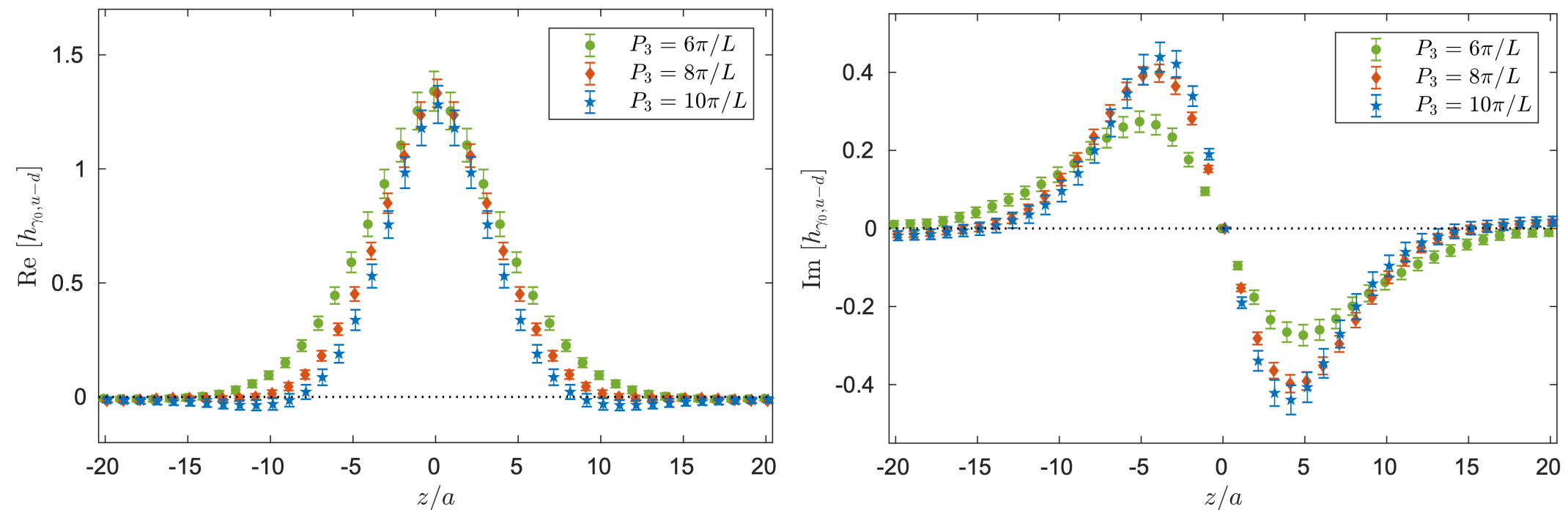
$$\tilde{q}_\Gamma(x, t, \xi, P_3, \mu) = \int_{-\infty}^{\infty} \frac{dz}{4\pi} e^{-ixP_3z} \langle N(P_f) | \bar{\Psi}(z) \Gamma \mathcal{W}(z, 0) \Psi(0) | N(P_i) \rangle_\mu$$

Limitations of lattice data

Matrix elements of non-local operators defined in coordinate space (z)

$$\mathcal{M}(P_f, P_i, z) = \langle N(P_f) | \bar{\Psi}(z) \Gamma \mathcal{W}(z, 0) \Psi(0) | N(P_i) \rangle_\mu$$

★ Lattice data limited by lattice size: $-\frac{L}{2} \leq z \leq \frac{L}{2}$



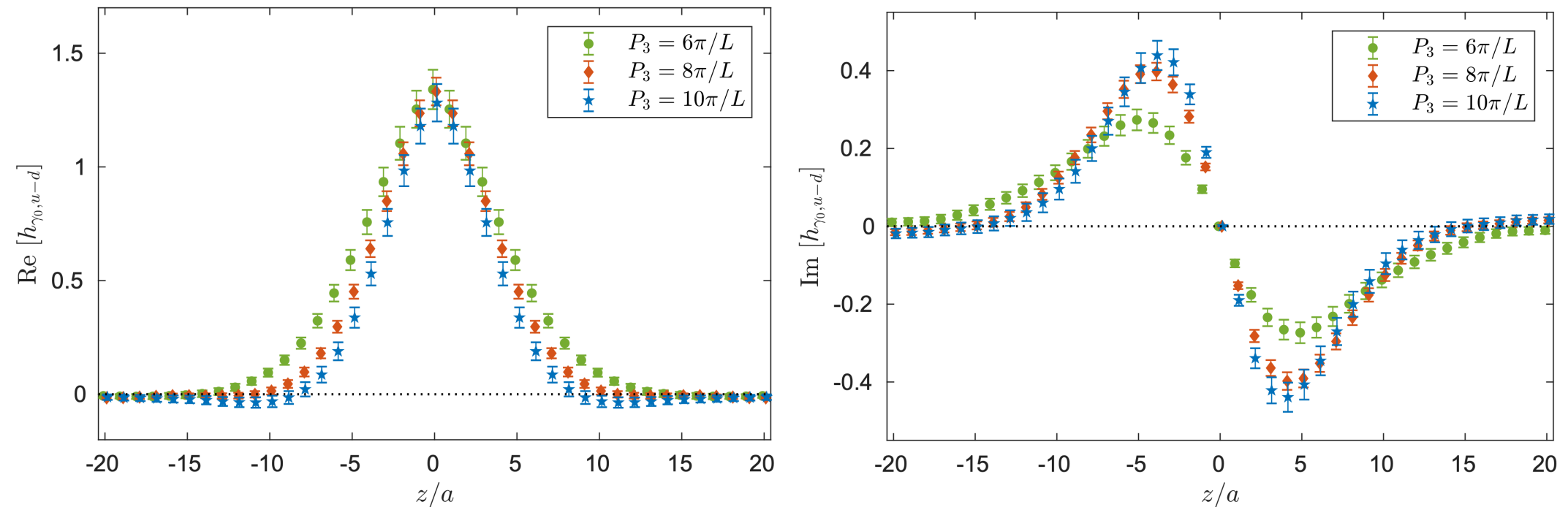
[C. Alexandrou et al. (ETMC), PRL 121 (2018) 112001, arXiv:1803.02685]

Limitations of lattice data

Matrix elements of non-local operators defined in coordinate space (z)

$$\mathcal{M}(P_f, P_i, z) = \langle N(P_f) | \bar{\Psi}(z) \Gamma \mathcal{W}(z, 0) \Psi(0) | N(P_i) \rangle_\mu$$

★ Lattice data limited by lattice size: $-\frac{L}{2} \leq z \leq \frac{L}{2}$



[C. Alexandrou et al. (ETMC), PRL 121 (2018) 112001, arXiv:1803.02685]

★ Discretized Fourier transform

$$\tilde{q}_\Gamma(x, t, \xi, P_3, \mu) = \int_{-\infty}^{\infty} \frac{dz}{4\pi} e^{-ixP_3z} \mathcal{M}(P_f, P_i, z)$$

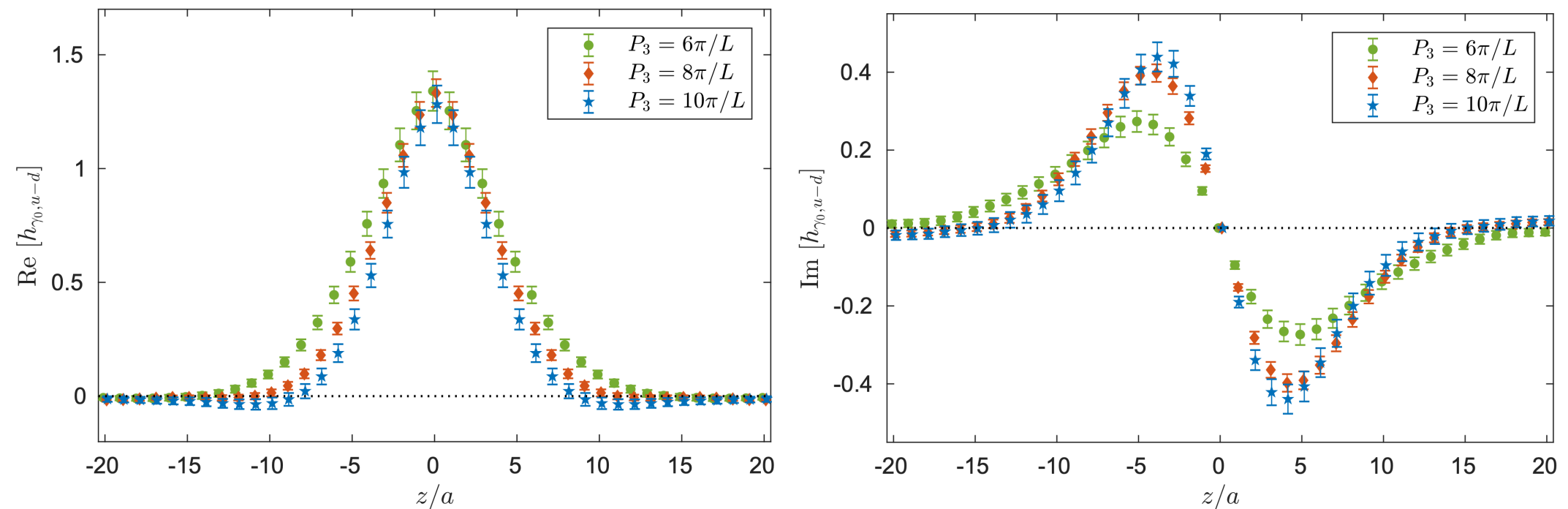
$$\int_{-\infty}^{\infty} dz \rightarrow \sum_{z=-z_{\max}}^{+z_{\max}}$$

Limitations of lattice data

Matrix elements of non-local operators defined in coordinate space (z)

$$\mathcal{M}(P_f, P_i, z) = \langle N(P_f) | \bar{\Psi}(z) \Gamma \mathcal{W}(z, 0) \Psi(0) | N(P_i) \rangle_\mu$$

★ Lattice data limited by lattice size: $-\frac{L}{2} \leq z \leq \frac{L}{2}$



[C. Alexandrou et al. (ETMC), PRL 121 (2018) 112001, arXiv:1803.02685]

★ Discretized Fourier transform

$$\tilde{q}_\Gamma(x, t, \xi, P_3, \mu) = \int_{-\infty}^{\infty} \frac{dz}{4\pi} e^{-ixP_3z} \mathcal{M}(P_f, P_i, z)$$

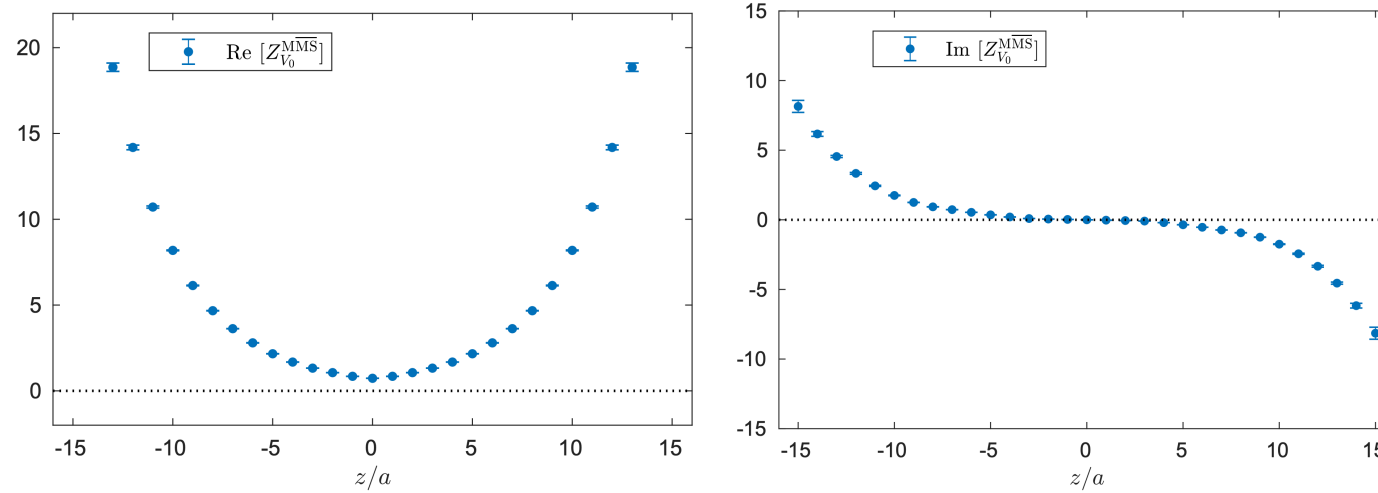
$$\int_{-\infty}^{\infty} dz \rightarrow \sum_{z=-z_{\max}}^{+z_{\max}}$$

ill-conditioned

Limitations of lattice data

- ★ Renormalization enhances systematics on data truncation

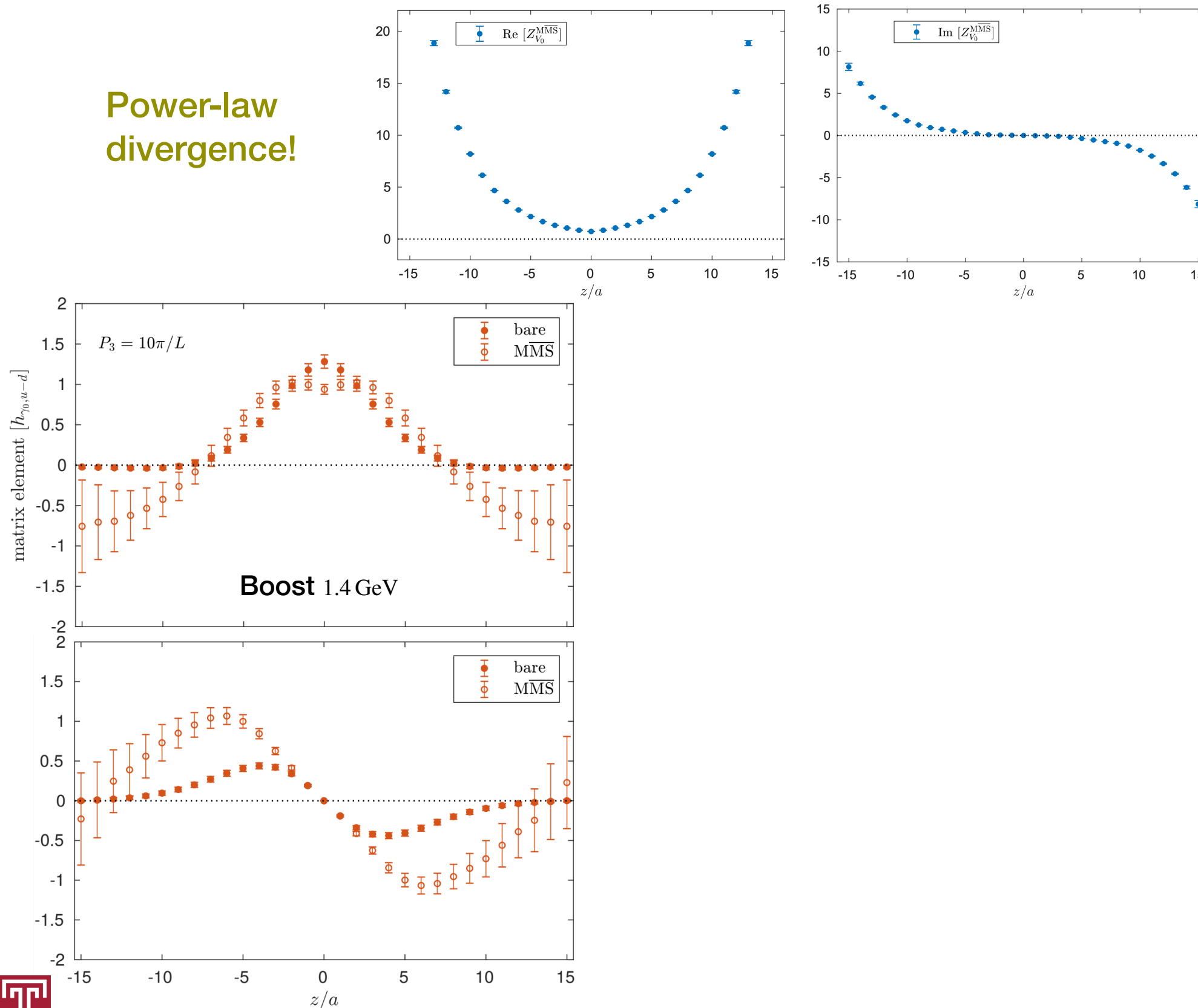
Power-law divergence!



Limitations of lattice data

★ Renormalization enhances systematics on data truncation

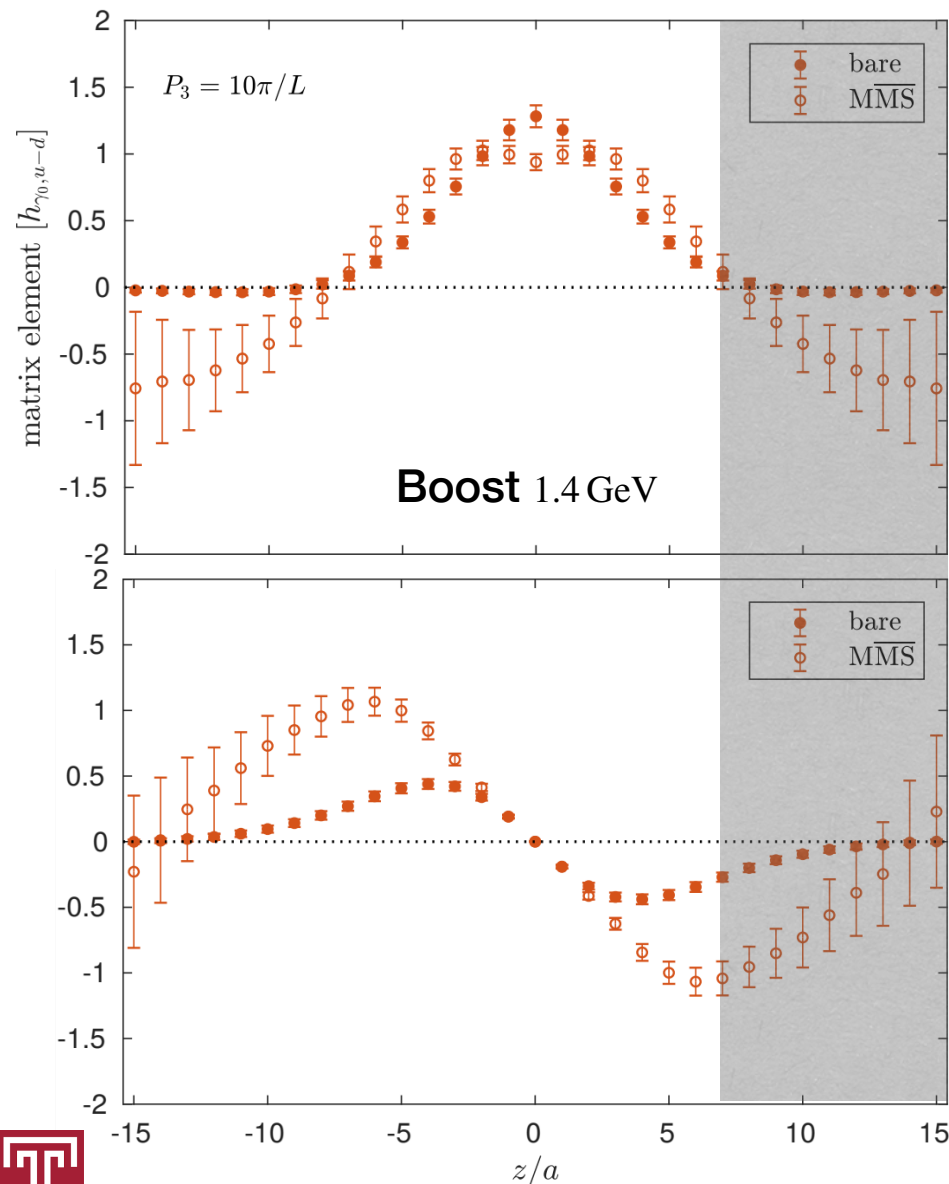
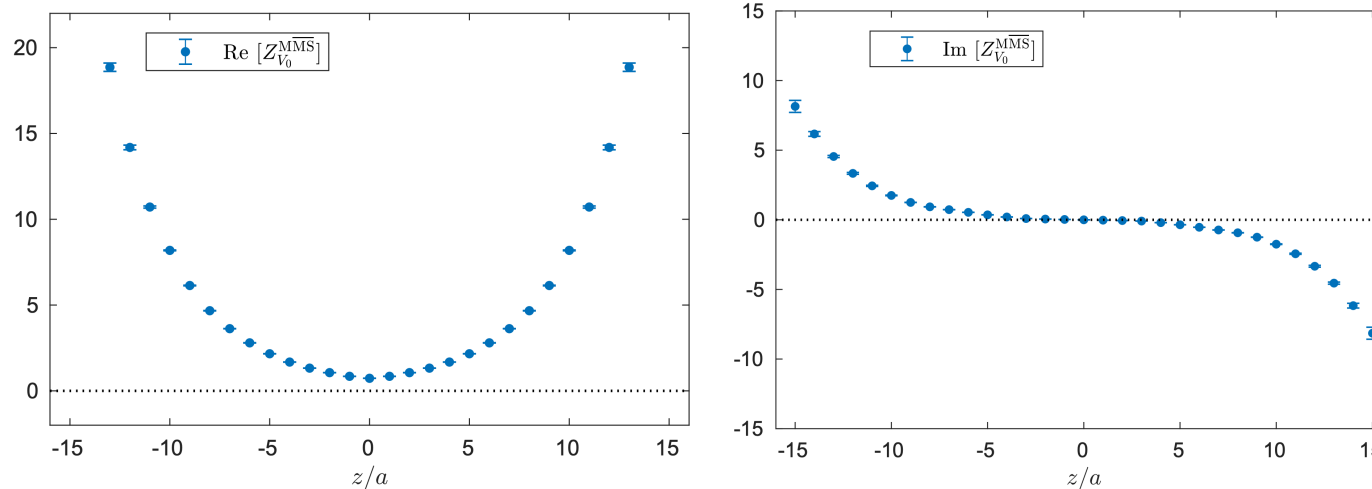
Power-law divergence!



Limitations of lattice data

- ★ Renormalization enhances systematics on data truncation

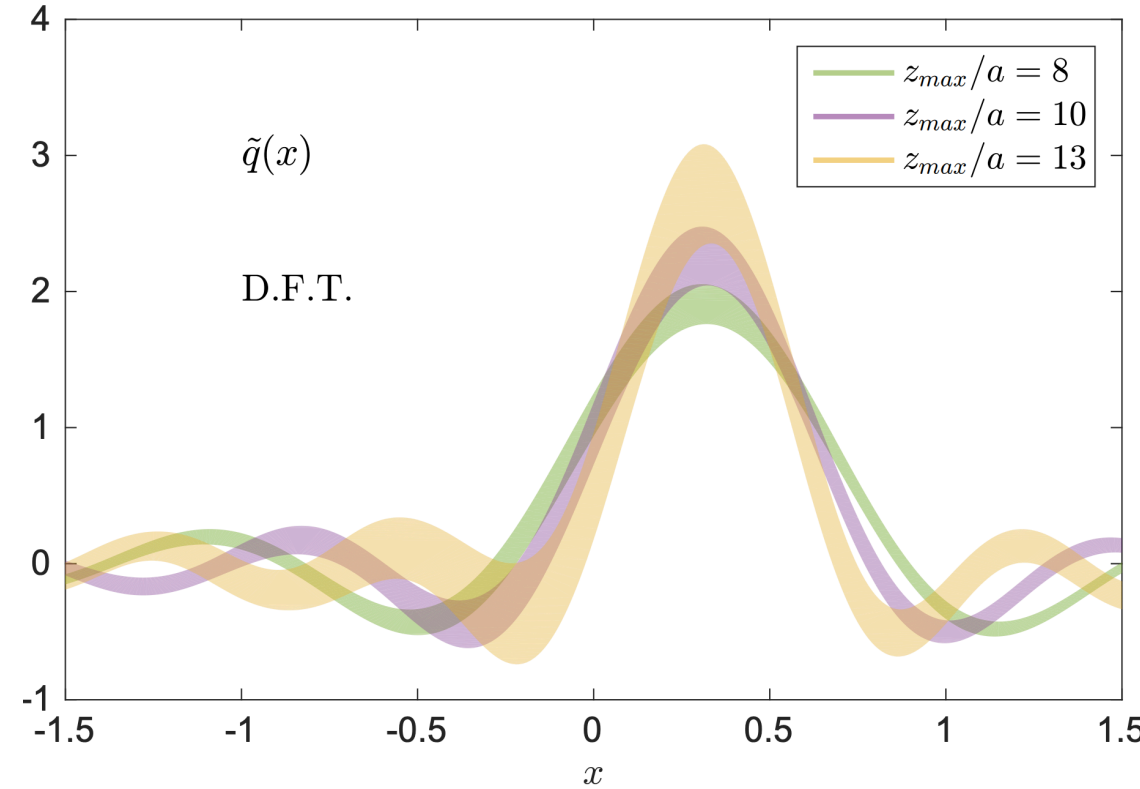
Power-law divergence!



- ★ Identification of appropriate cut is non-trivial
- ★ Omitted data contain information for the reconstruction.
- ★ Naive Fourier transform problematic as it relies on assumptions about the matrix elements
(Not unique solution to the inverse problem)

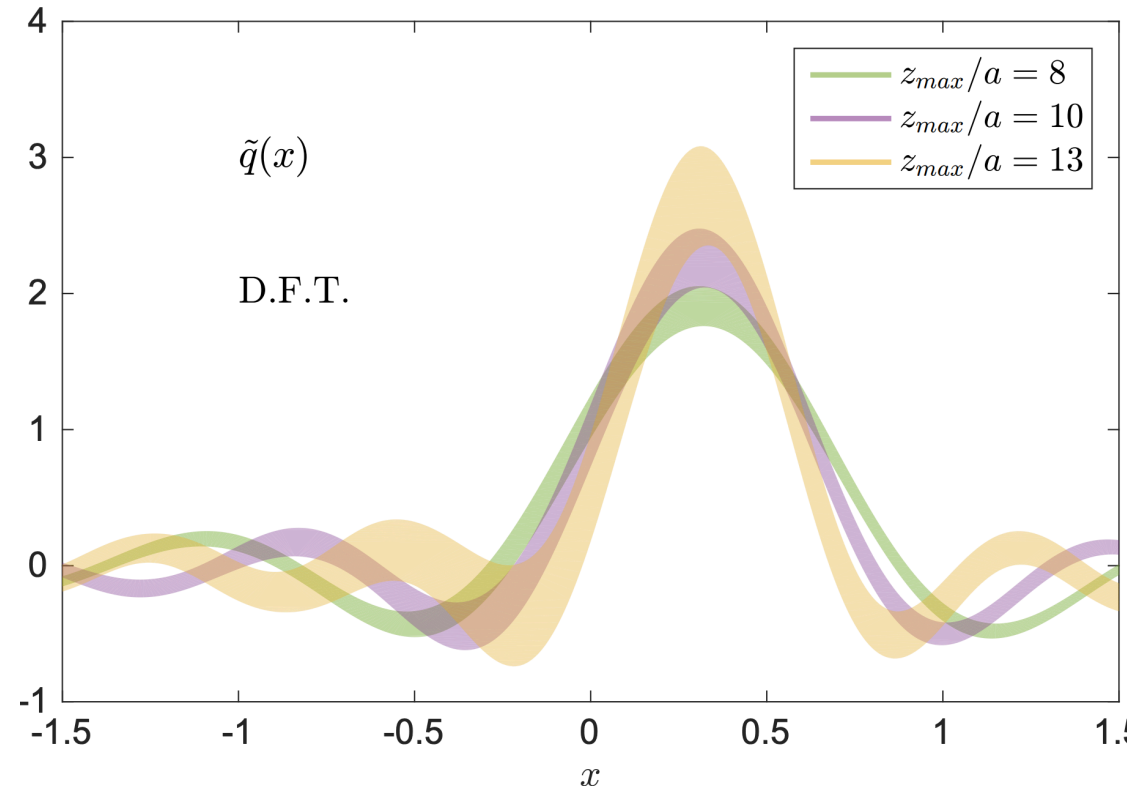
Limitations of lattice data

- ★ Discretized Fourier transform neglects contributions for $|z| > z_{\max}$



Limitations of lattice data

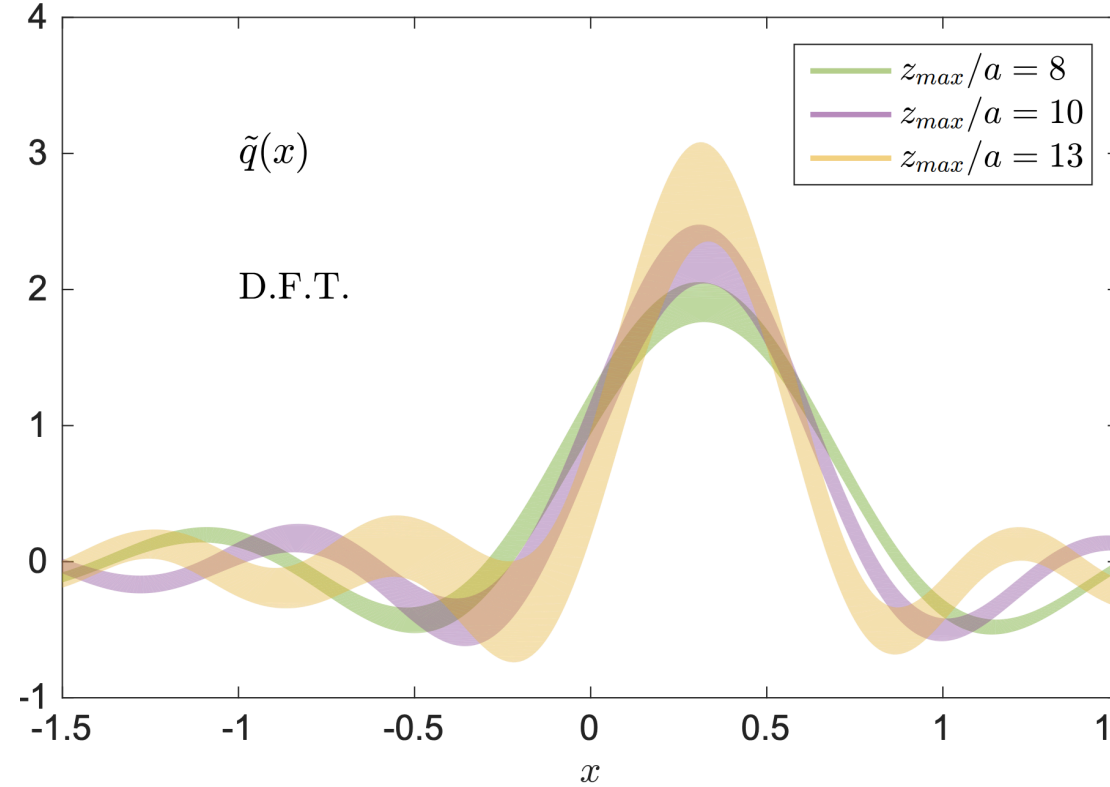
- ★ Discretized Fourier transform neglects contributions for $|z| > z_{\max}$



Periodicity of Fourier transform
leads to oscillatory behavior

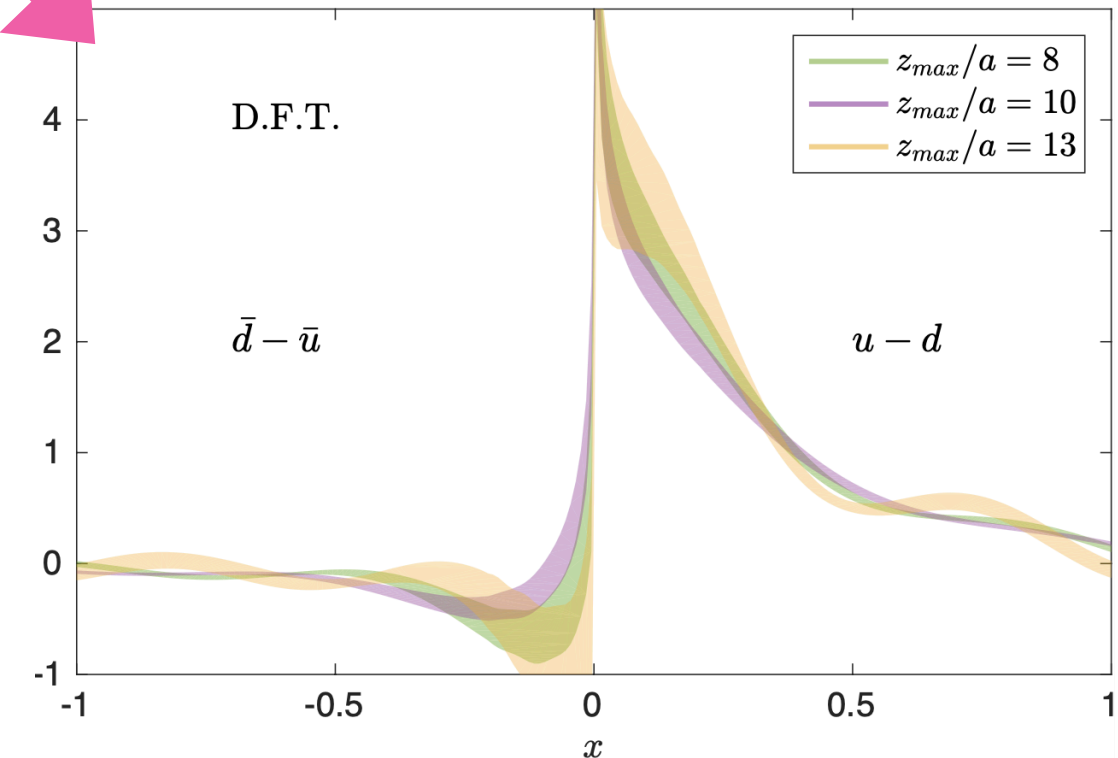
Limitations of lattice data

- ★ Discretized Fourier transform neglects contributions for $|z| > z_{\max}$



Periodicity of Fourier transform
leads to oscillatory behavior

- ★ Unphysical oscillations propagate to final PDFs



Alternative approaches to Fourier transform

Backus Gilbert

[G. Backus and F. Gilbert, Geophysical Journal International 16, 169 (1968)]

[J. Karpie, K. Orginos, and S. Zafeiropoulos, JHEP 11, 178 (2018), arXiv:1807.10933] (implementation)

- A model-independent criterion for reconstruction:
minimal variance of solution with respect to statistical variation of input data
- Reconstruction applied separately for each value of x
- Separation of FT in sine and cosine parts

$$\tilde{q}(x, \mu_0, P_3) = \frac{1}{2} \sum_{z/a} \left(a_{\cos}(x)_{z/a} \operatorname{Re} [\mathcal{M}(z, P_3, \mu_0)] + a_{\sin}(x)_{z/a} \operatorname{Im} [\mathcal{M}(z, P_3, \mu_0)] \right)$$

Backus Gilbert

[G. Backus and F. Gilbert, Geophysical Journal International 16, 169 (1968)]

[J. Karpie, K. Orginos, and S. Zafeiropoulos, JHEP 11, 178 (2018), arXiv:1807.10933] (implementation)

- A model-independent criterion for reconstruction:
minimal variance of solution with respect to statistical variation of input data
- Reconstruction applied separately for each value of x
- Separation of FT in sine and cosine parts

$$\tilde{q}(x, \mu_0, P_3) = \frac{1}{2} \sum_{z/a} \left(a_{\cos}(x)_{z/a} \operatorname{Re} [\mathcal{M}(z, P_3, \mu_0)] + a_{\sin}(x)_{z/a} \operatorname{Im} [\mathcal{M}(z, P_3, \mu_0)] \right)$$

- ★ At each x , a vector $a_K(x)$ is defined as an approximate inverse of kernel function $K(x)$. $a_K(x)$ identified from optimization conditions based on BG criterion

$$\Delta(x - x') = \sum_{z/a=0}^{d-1} a_K(x)_{z/a} K(x')_{z/a}$$

$$K(x')_{z/a} = \cos(x' P_3 z), \sin(x' P_3 z)$$

d : number of input data

- ★ $\Delta(x - x')$ approximates Dirac delta function with minimized width.
Quality of approximation depends on d

Backus Gilbert

[G. Backus and F. Gilbert, Geophysical Journal International 16, 169 (1968)]

[J. Karpie, K. Orginos, and S. Zafeiropoulos, JHEP 11, 178 (2018), arXiv:1807.10933] (implementation)

★ Width minimization leads to

$$\mathbf{a}_K(x) = \frac{\mathbf{M}_K^{-1}(x) \mathbf{u}_K}{\mathbf{u}_K^T \mathbf{M}_K^{-1}(x) \mathbf{u}_K}$$

where

$$M_K(x)_{\nu\nu'} = \int_0^1 dx' (x - x')^2 K(x')_\nu K(x')_{\nu'} + \rho \delta_{\nu\nu'}$$

$$u_{K\nu} = \int_0^1 dx' K(x')_\nu$$

Backus Gilbert

[G. Backus and F. Gilbert, Geophysical Journal International 16, 169 (1968)]

[J. Karpie, K. Orginos, and S. Zafeiropoulos, JHEP 11, 178 (2018), arXiv:1807.10933] (implementation)

- ★ Width minimization leads to

$$\mathbf{a}_K(x) = \frac{\mathbf{M}_K^{-1}(x) \mathbf{u}_K}{\mathbf{u}_K^T \mathbf{M}_K^{-1}(x) \mathbf{u}_K}$$

where $M_K(x)_{\nu\nu'} = \int_0^1 dx' (x - x')^2 K(x')_\nu K(x')_{\nu'} + \rho \delta_{\nu\nu'}$ $u_{K\nu} = \int_0^1 dx' K(x')_\nu$

- ★ ρ regularizes matrix to make it invertible (Tikhonov)
- ★ Empirical value $\rho = 10^{-3}$
- ★ Smaller ρ values introduce large oscillations in reconstructed PDF due to very small eigenvalues of $M_K(x)$

Backus Gilbert

[G. Backus and F. Gilbert, Geophysical Journal International 16, 169 (1968)]

[J. Karpie, K. Orginos, and S. Zafeiropoulos, JHEP 11, 178 (2018), arXiv:1807.10933] (implementation)

- ★ Width minimization leads to

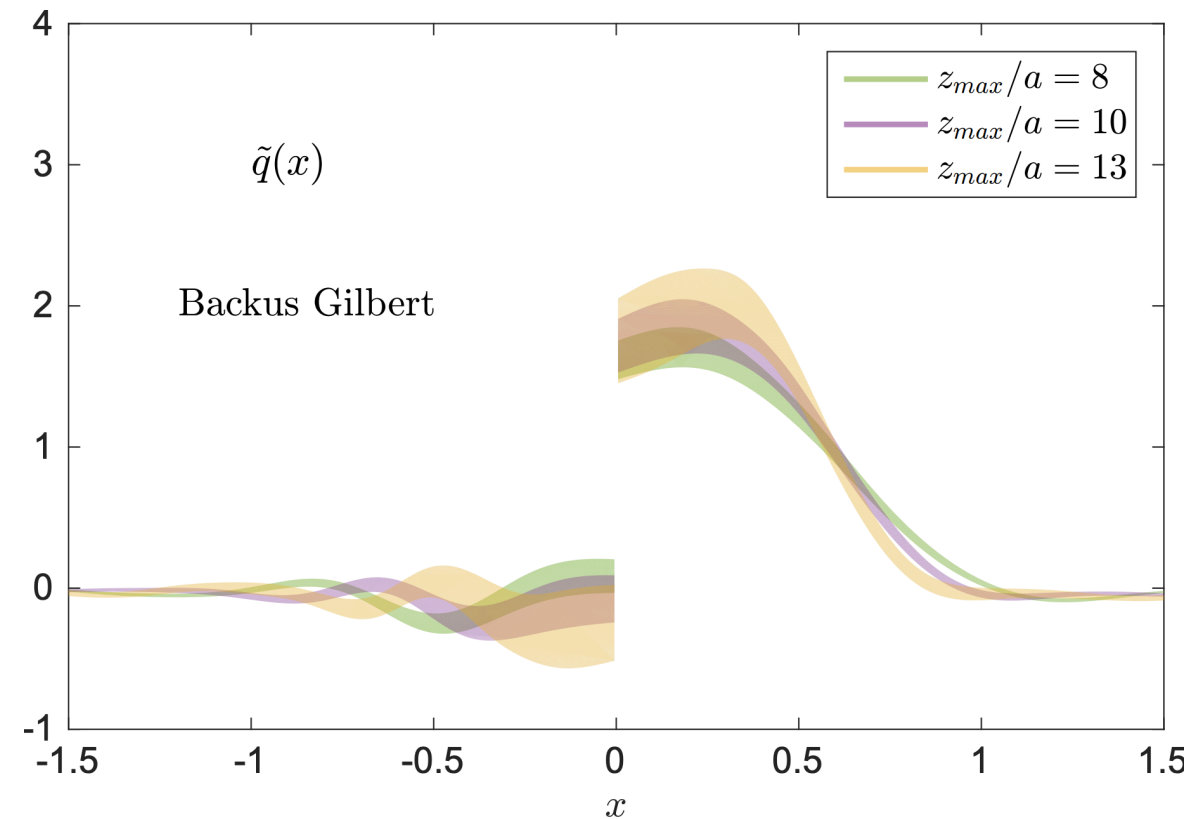
$$\mathbf{a}_K(x) = \frac{\mathbf{M}_K^{-1}(x) \mathbf{u}_K}{\mathbf{u}_K^T \mathbf{M}_K^{-1}(x) \mathbf{u}_K}$$

where $M_K(x)_{\nu\nu'} = \int_0^1 dx' (x - x')^2 K(x')_\nu K(x')_{\nu'} + \rho \delta_{\nu\nu'}$ $u_{K\nu} = \int_0^1 dx' K(x')_\nu$

- ★ ρ regularizes matrix to make it invertible (Tikhonov)
- ★ Empirical value $\rho = 10^{-3}$
- ★ Smaller ρ values introduce large oscillations in reconstructed PDF due to very small eigenvalues of $M_K(x)$

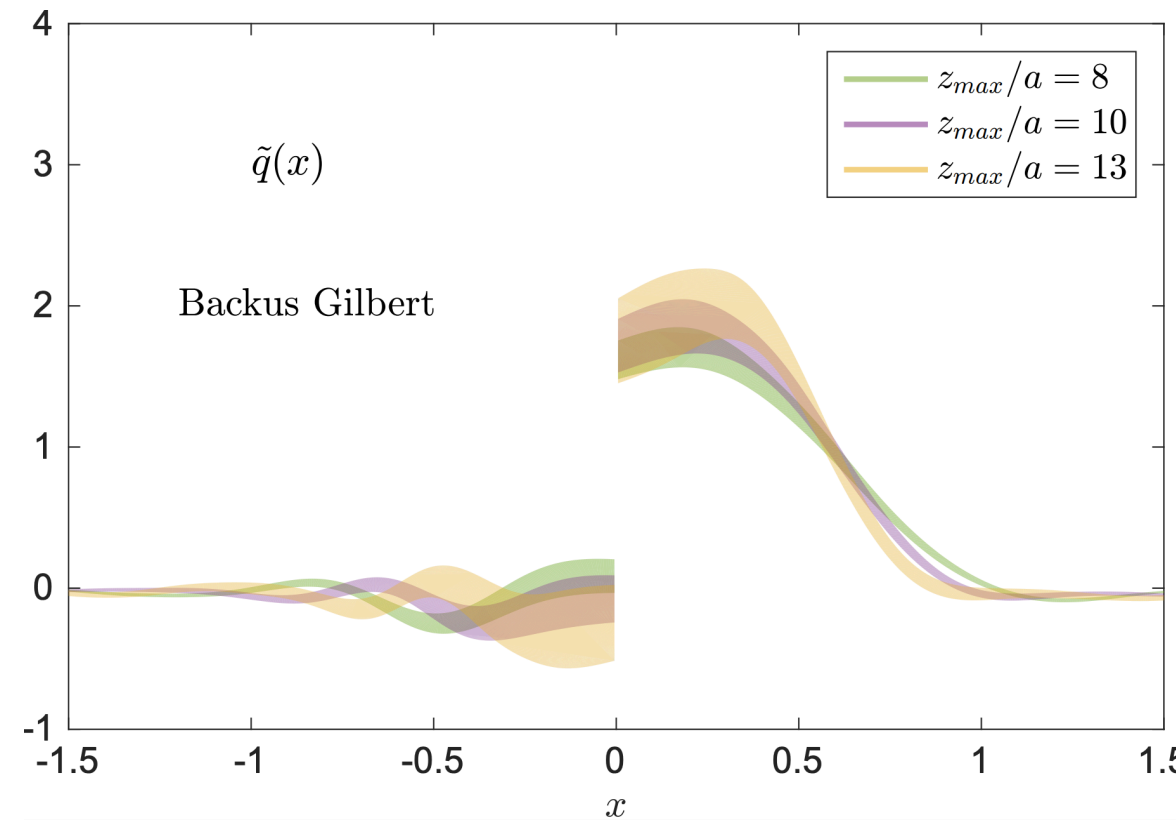
BG with preconditioning alternative approach
(Rescaling, $K(x) \rightarrow p(x)K(x)$, $q(x) \rightarrow q(x)/p(x)$)

Backus Gilbert



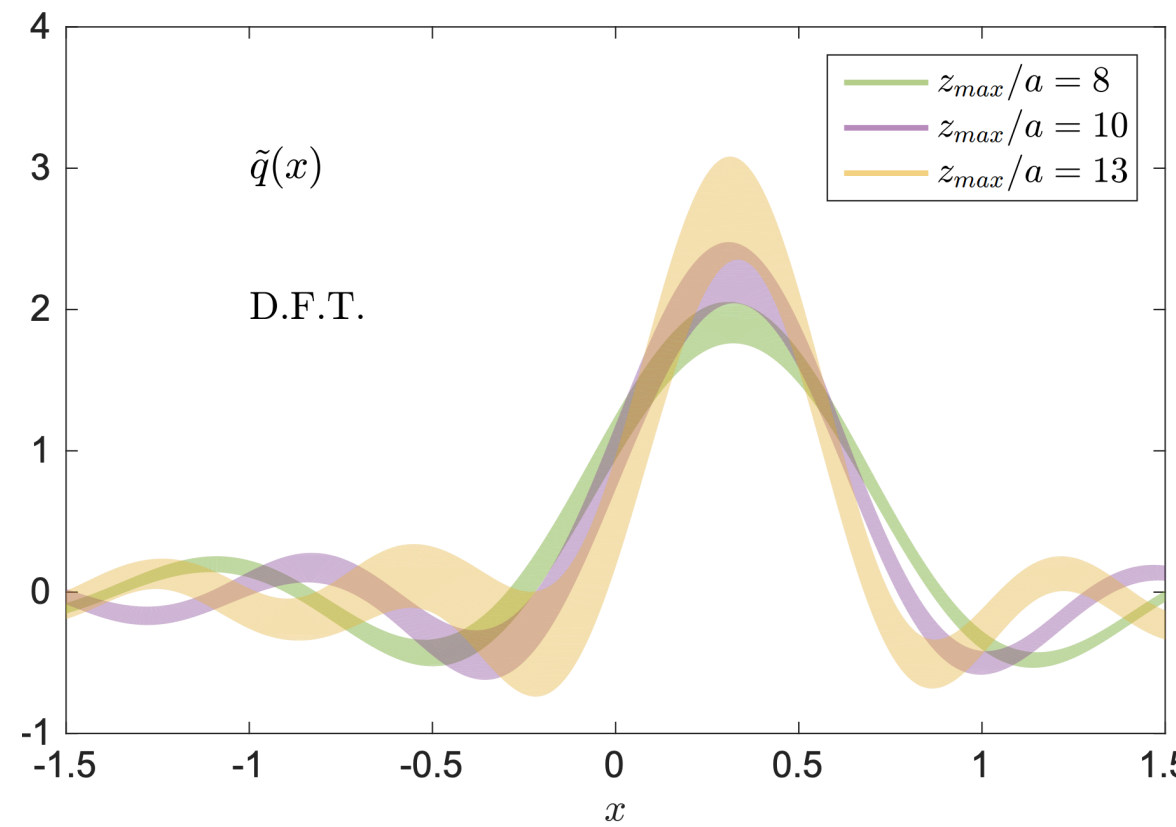
- ★ Convergence of results at about $d = 11$
- ★ Unphysical oscillations are negligible in the quark region

Backus Gilbert



★ Convergence of results at about $d = 11$

★ Unphysical oscillations are negligible in the quark region



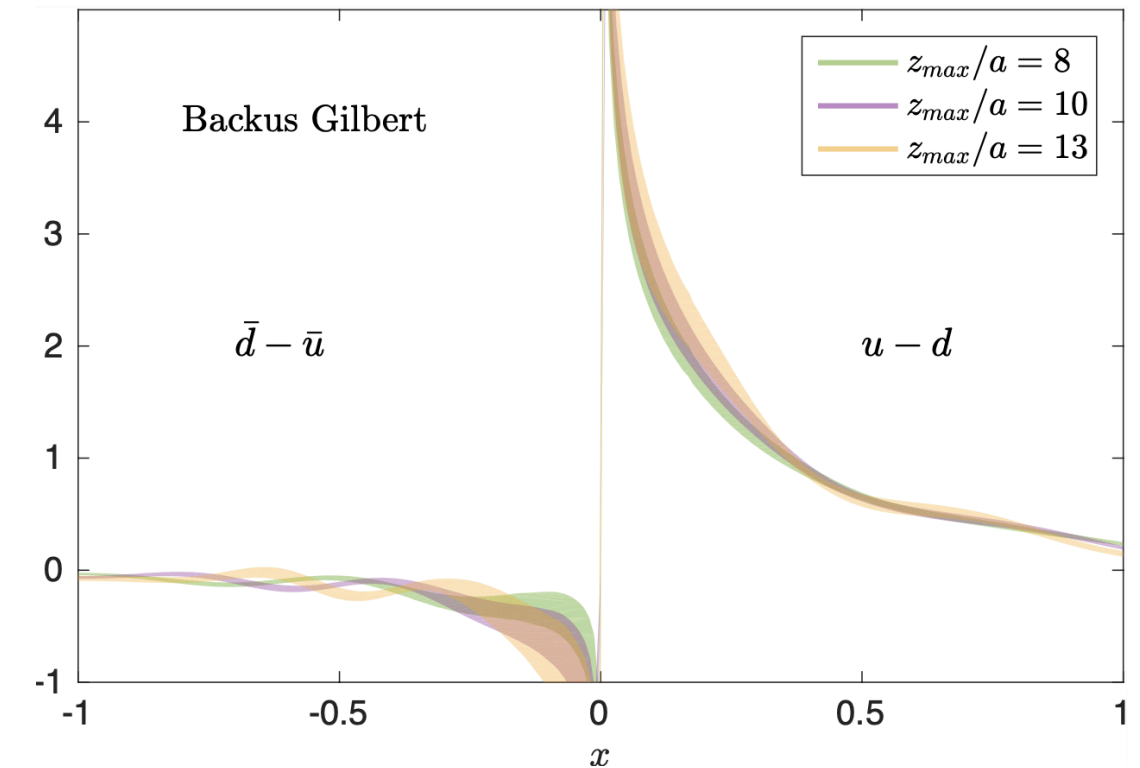
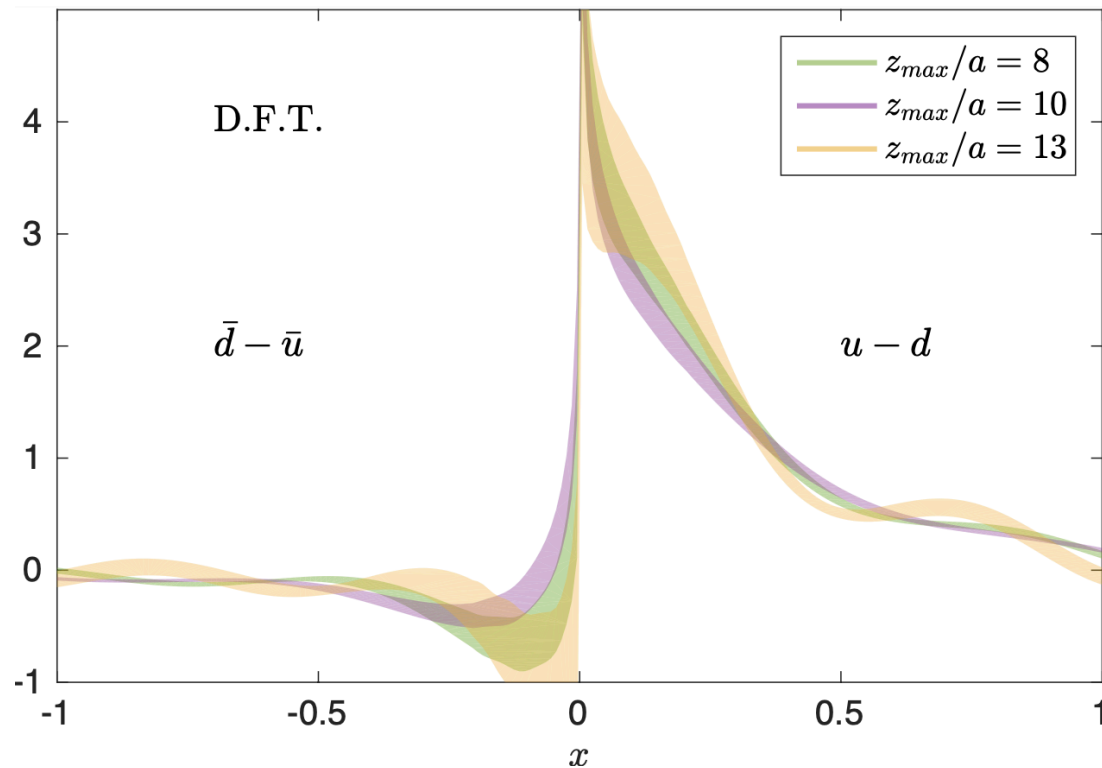
★ Standard FT: quasi-PDF is bound to be negative if matrix elements entering the transforms do not decay to zero fast enough.

Backus Gilbert

How does the addition of lattice data affect the final PDF as obtained from FT and BG reconstructions?

Backus Gilbert

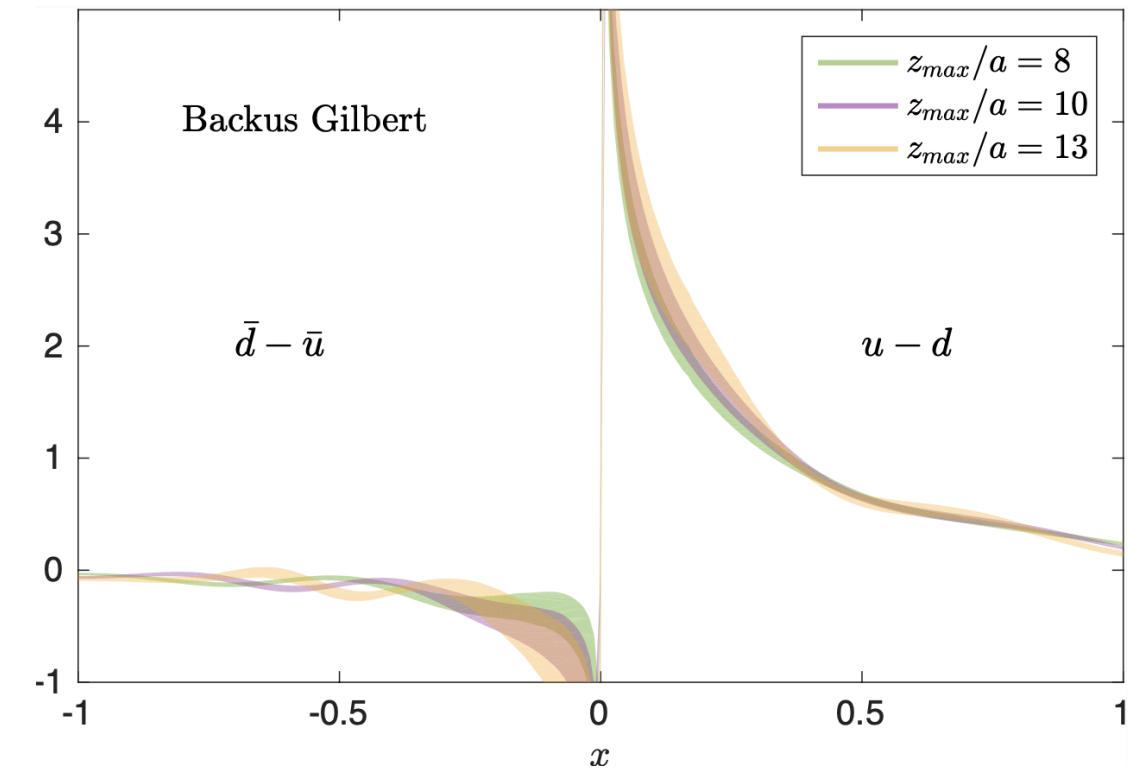
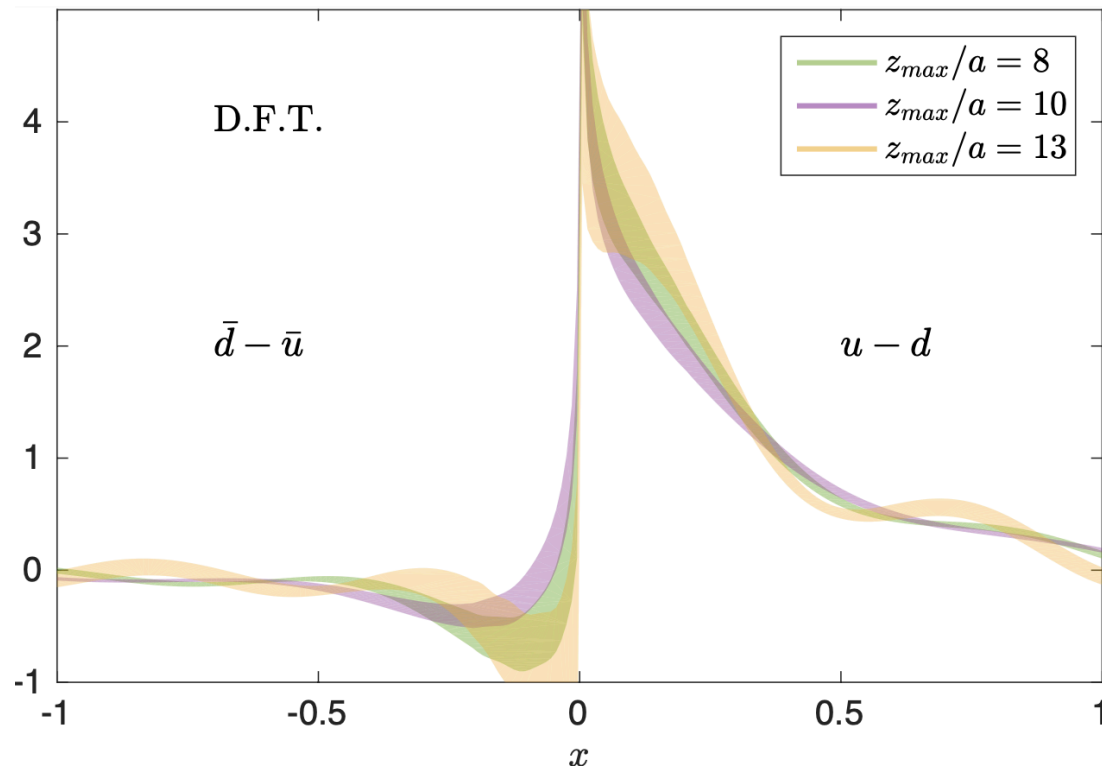
How does the addition of lattice data affect the final PDF as obtained from FT and BG reconstructions?



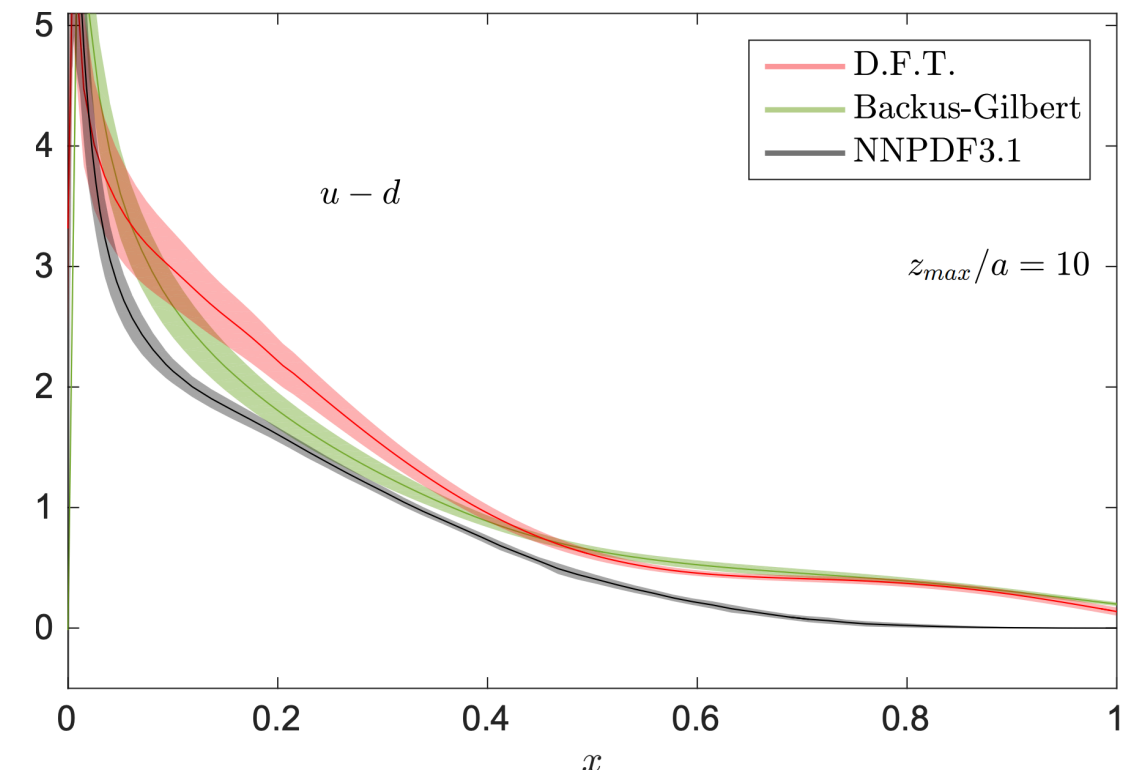
- ★ Larger deviations in standard FT

Backus Gilbert

How does the addition of lattice data affect the final PDF as obtained from FT and BG reconstructions?

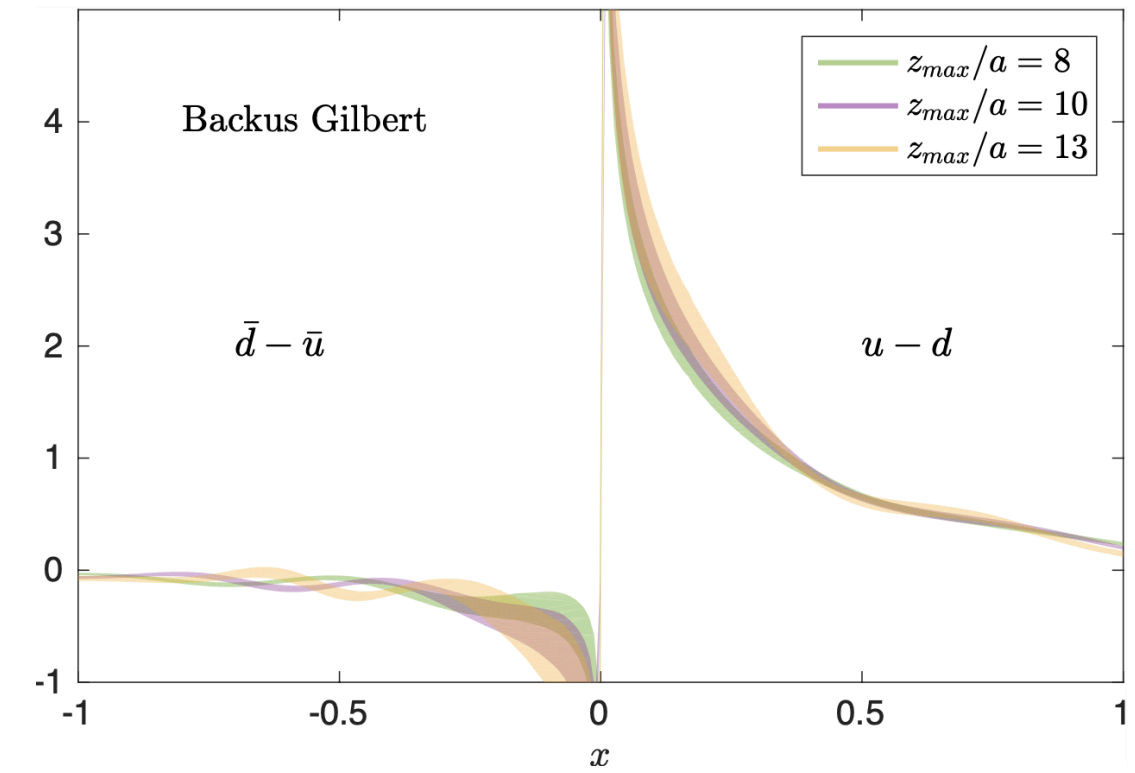
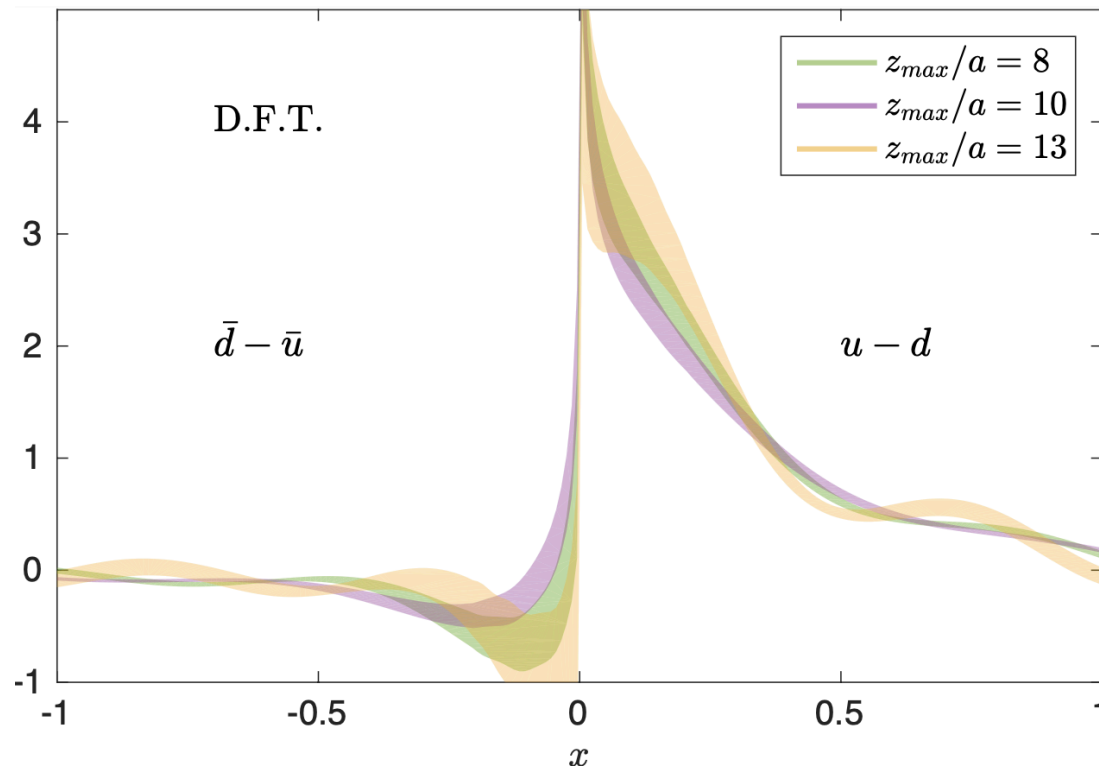


- ★ Larger deviations in standard FT
- ★ Small improvement in BG approach



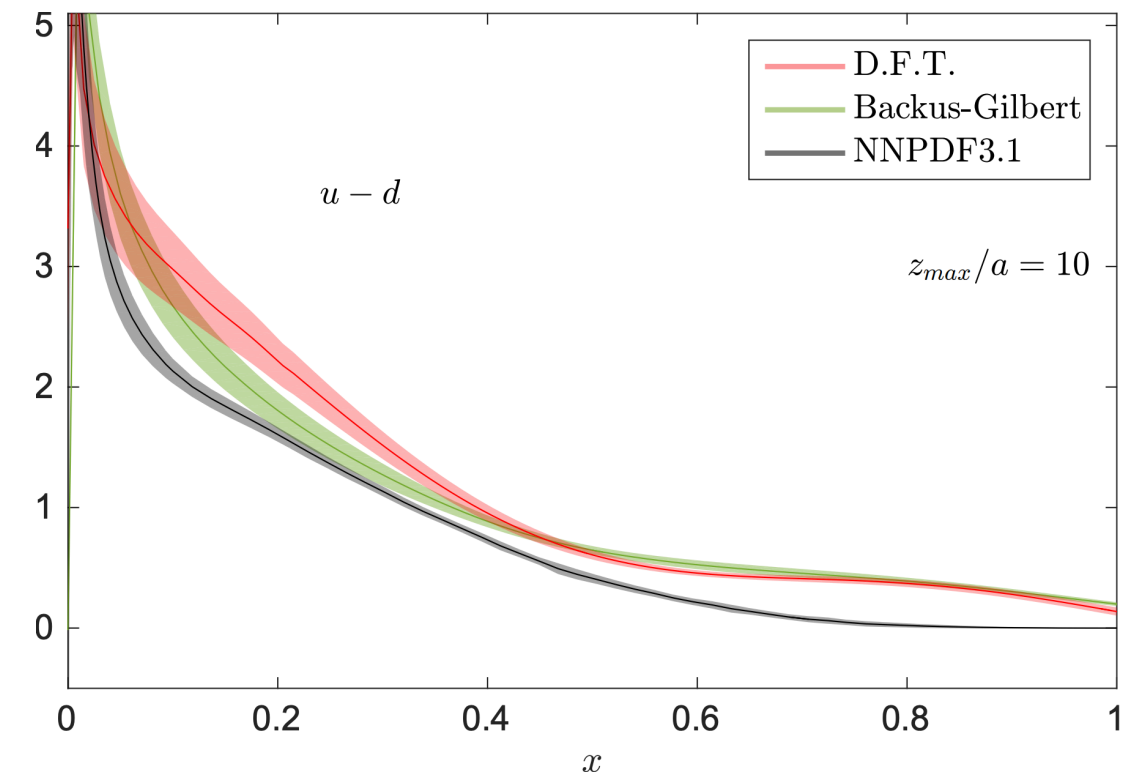
Backus Gilbert

How does the addition of lattice data affect the final PDF as obtained from FT and BG reconstructions?



- ★ Larger deviations in standard FT
- ★ Small improvement in BG approach

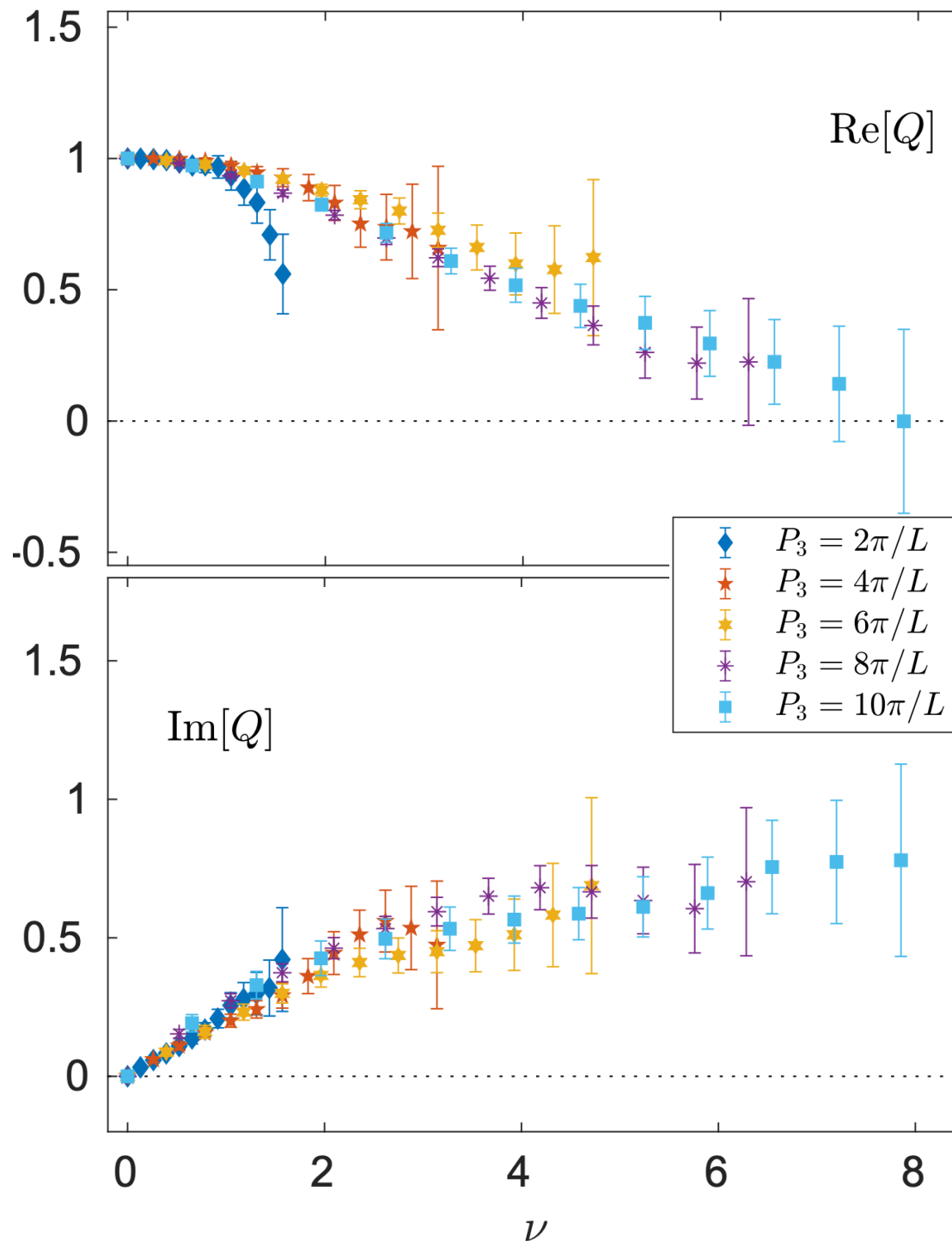
Further increase of data set requires simulations using large-volume ensembles and finer lattice spacing



Alternative methods for distribution functions (pseudo-PDFs)

pseudo-PDFs

[A. Radyushkin, Phys. Rev. D96 (2017) 034025]



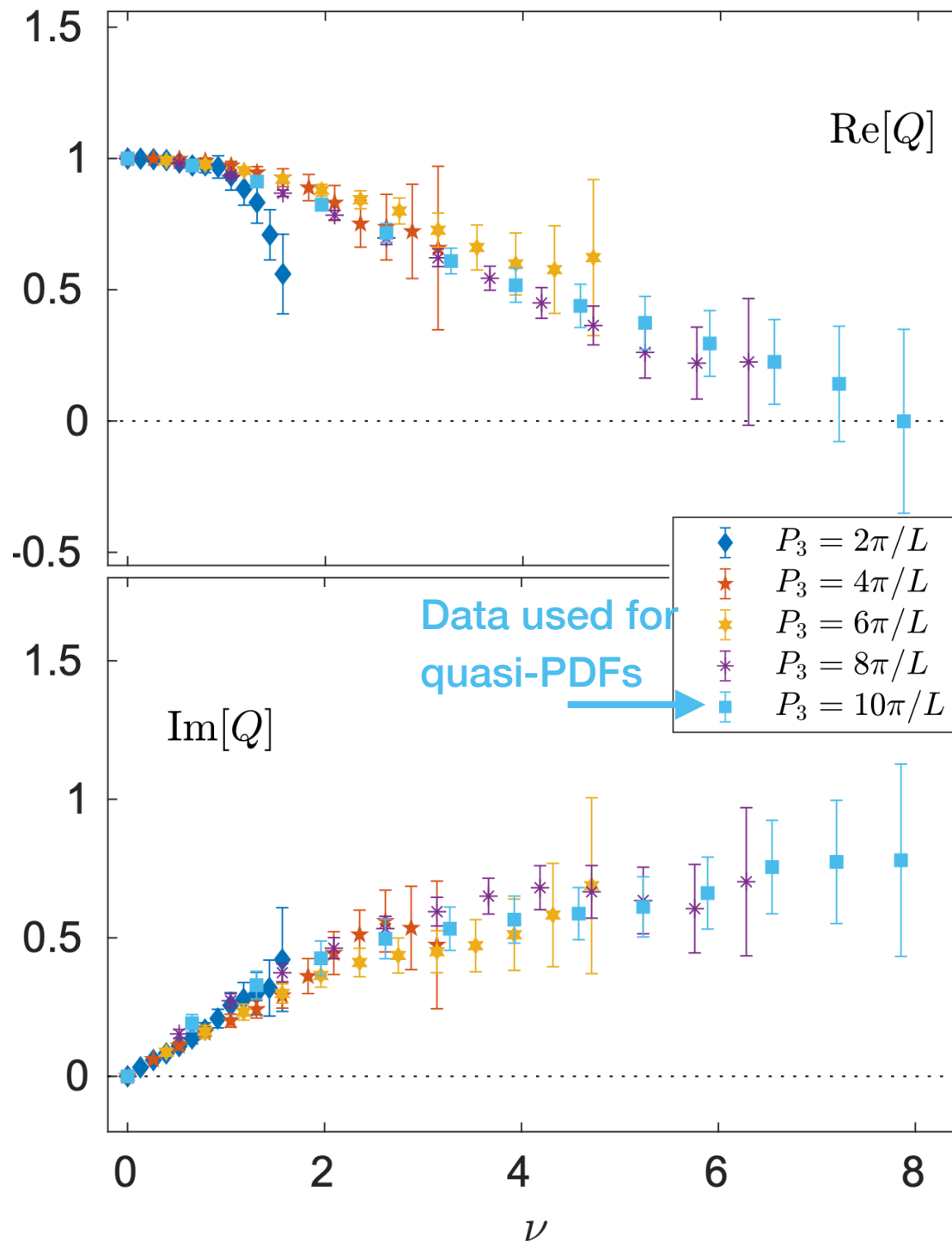
- ★ Reduced Ioffe-time distributions (ITD)
(renormalization scheme)
- ★ Practical advantage: all values of P_3
analyzed simultaneously

$$\mathfrak{M}(\nu, z^2) = \frac{\mathcal{M}(\nu, z^2) / \mathcal{M}(\nu, 0)}{\mathcal{M}(0, z^2) / \mathcal{M}(0, 0)} \quad (\nu = z \cdot P_3)$$

[M. Bhat et al. (ETMC) PRD 103 (2021) 3, 034510, arXiv:2005.02102]

pseudo-PDFs

[A. Radyushkin, Phys. Rev. D96 (2017) 034025]



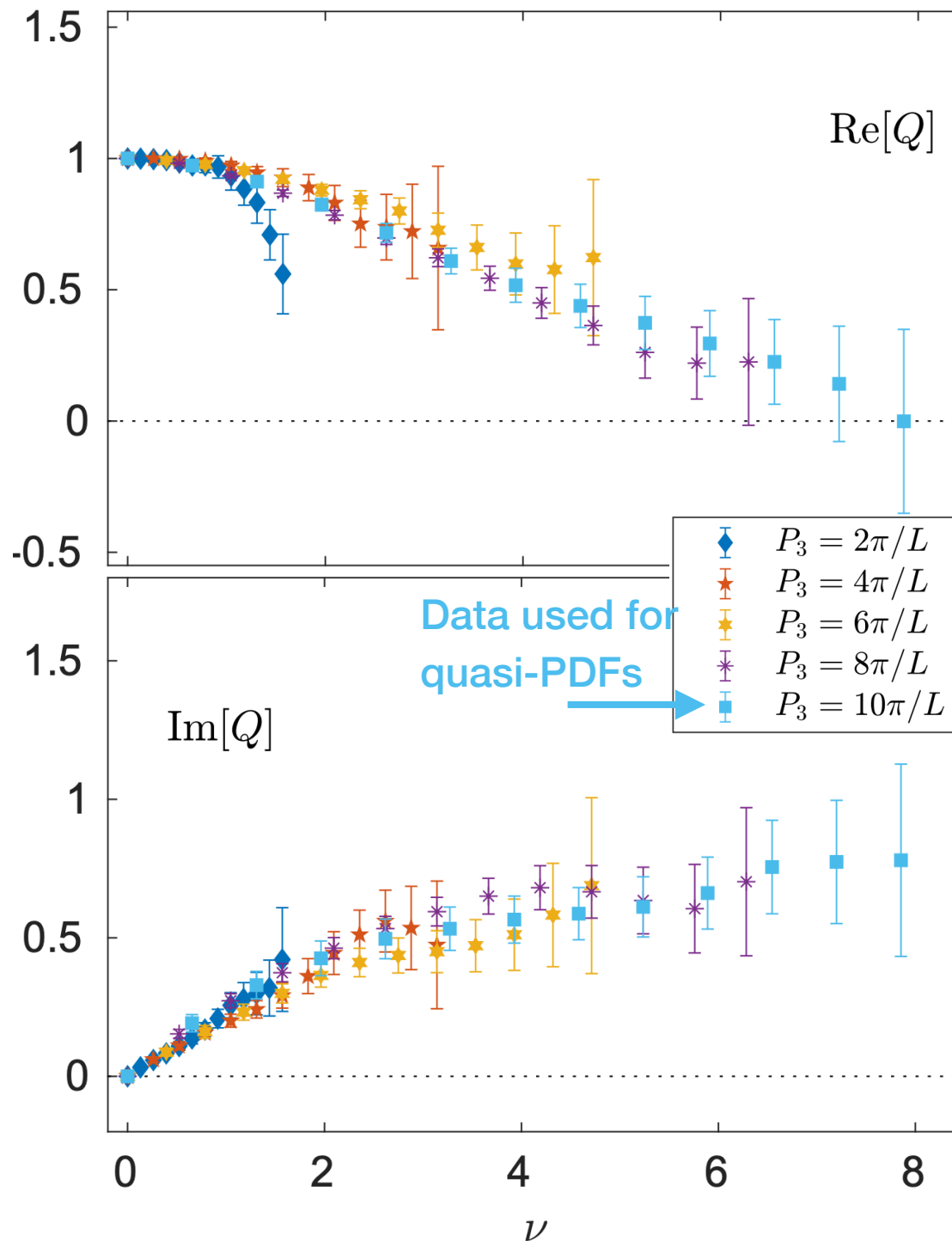
- ★ Reduced Ioffe-time distributions (ITD)
(renormalization scheme)
- ★ Practical advantage: all values of P_3
analyzed simultaneously

$$\mathfrak{M}(\nu, z^2) = \frac{\mathcal{M}(\nu, z^2) / \mathcal{M}(\nu, 0)}{\mathcal{M}(0, z^2) / \mathcal{M}(0, 0)} \quad (\nu = z \cdot P_3)$$

[M. Bhat et al. (ETMC) PRD 103 (2021) 3, 034510, arXiv:2005.02102]

pseudo-PDFs

[A. Radyushkin, Phys. Rev. D96 (2017) 034025]



★ Reduced Ioffe-time distributions (ITD)
(renormalization scheme)

★ Practical advantage: all values of P_3
analyzed simultaneously

$$\mathfrak{M}(\nu, z^2) = \frac{\mathcal{M}(\nu, z^2) / \mathcal{M}(\nu, 0)}{\mathcal{M}(0, z^2) / \mathcal{M}(0, 0)} \quad (\nu = z \cdot P_3)$$

★ Inverse problem present

$$Q(\nu, \mu^2) = \int_{-1}^1 dx e^{i\nu x} q(x, \mu^2)$$

[M. Bhat et al. (ETMC) PRD 103 (2021) 3, 034510, arXiv:2005.02102]

pseudo-PDFs

[A. Radyushkin, Phys. Rev. D96 (2017) 034025]

- ★ Alternative reconstruction technique: **fitting ansatz**

[B. Joo et. al, JHEP 12, 081, arXiv:1908.09771]

$$q(x) = Nx^a(1-x)^b$$

- ★ a, b fitting parameters, N normalization or free parameter

- ★ Fits performed minimizing the χ^2 function where

σ_Q is statistical error of Q ,

Q_f is FT of the ansatz for $q(x)$

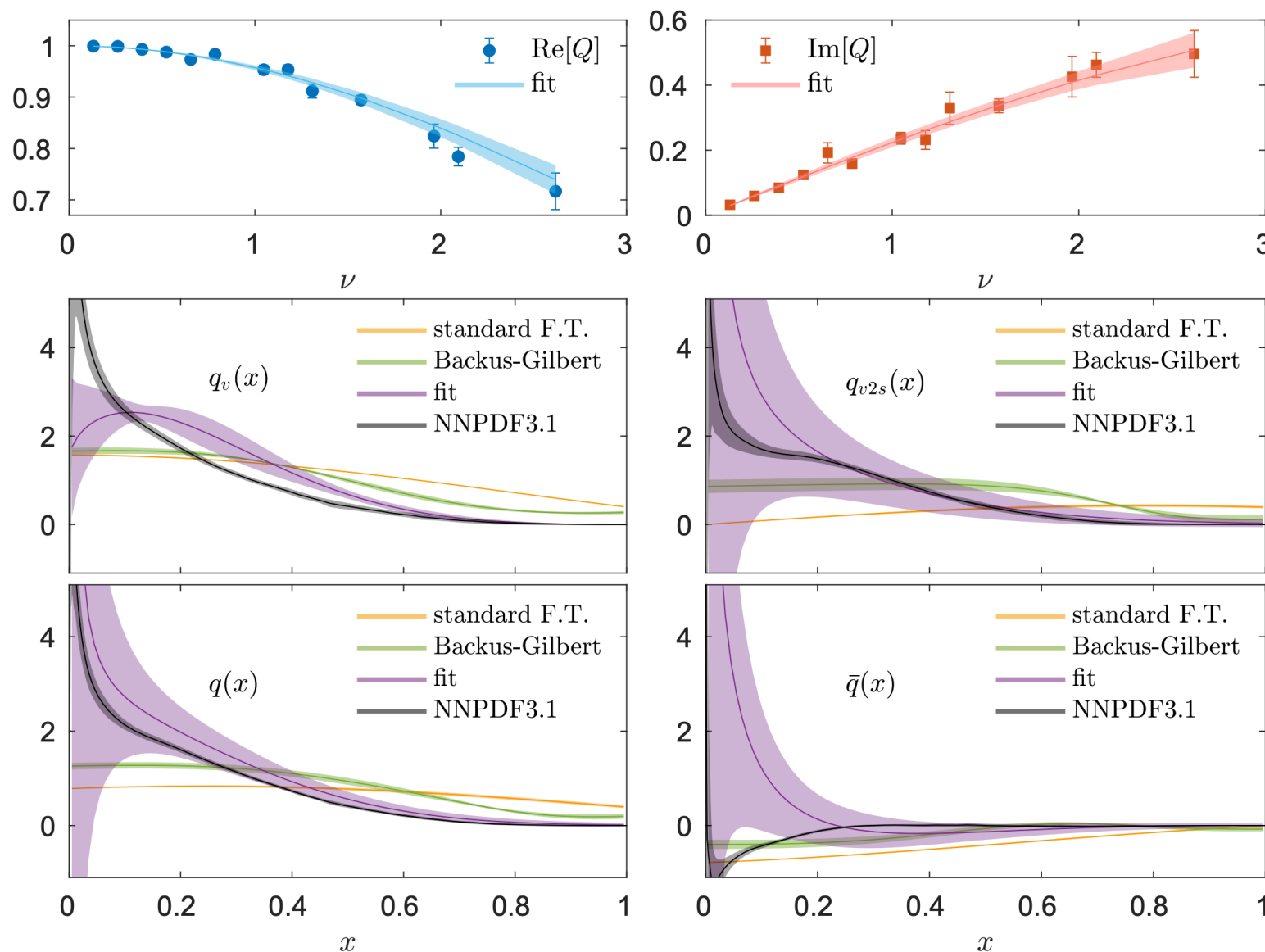
$$Q(\nu, \mu^2) = \int_{-1}^1 dx e^{i\nu x} q(x, \mu^2)$$

$$\chi^2 = \sum_{\nu=0}^{\nu_{\max}} \frac{Q(\nu, \mu^2) - Q_f(\nu, \mu^2)}{\sigma_Q^2(\nu, \mu^2)}$$

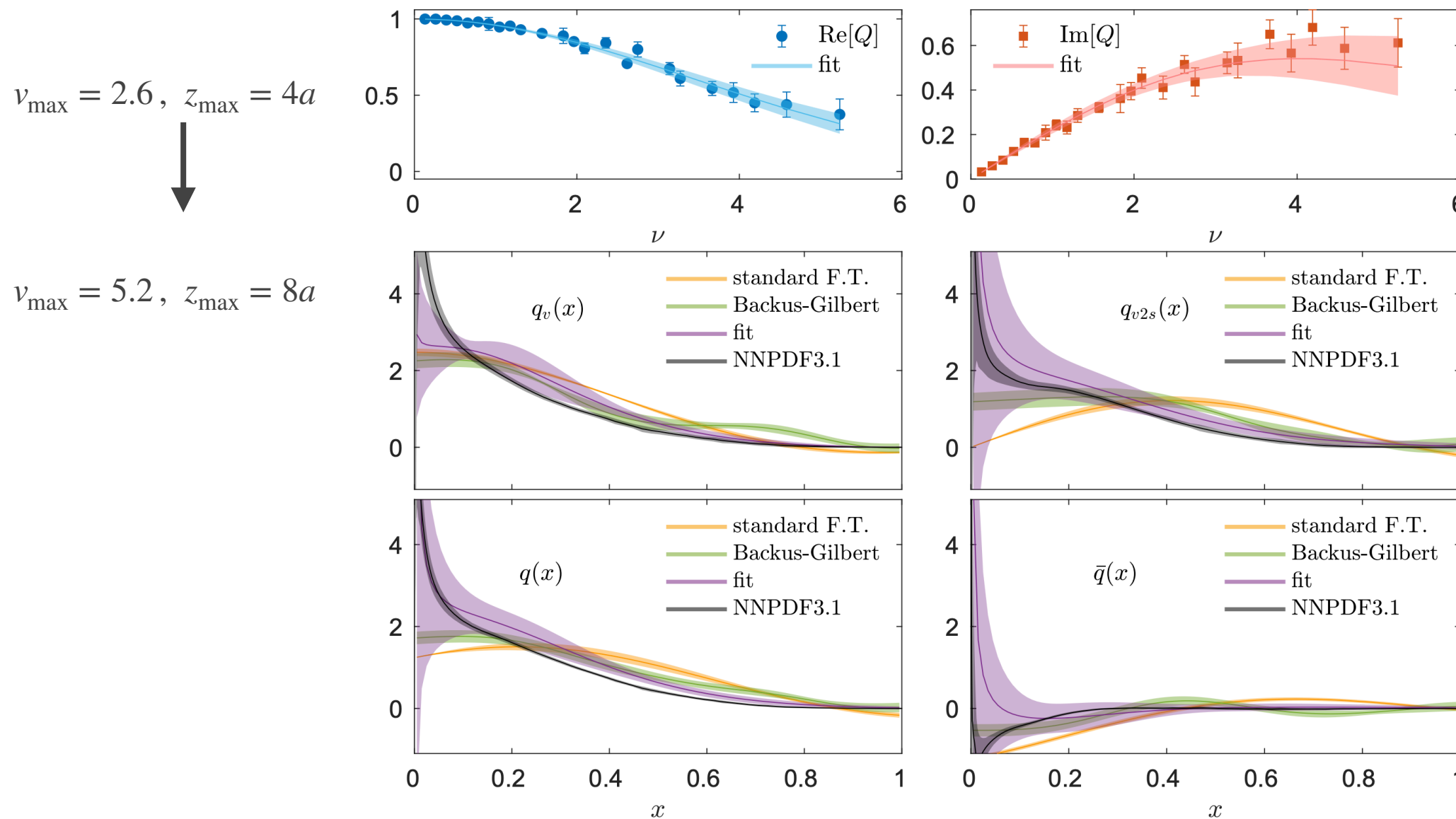
- ★ The fitted function is continuous and reconstruction is not subject to inverse problem (other systematic effects present)

Comparison of reconstruction methods

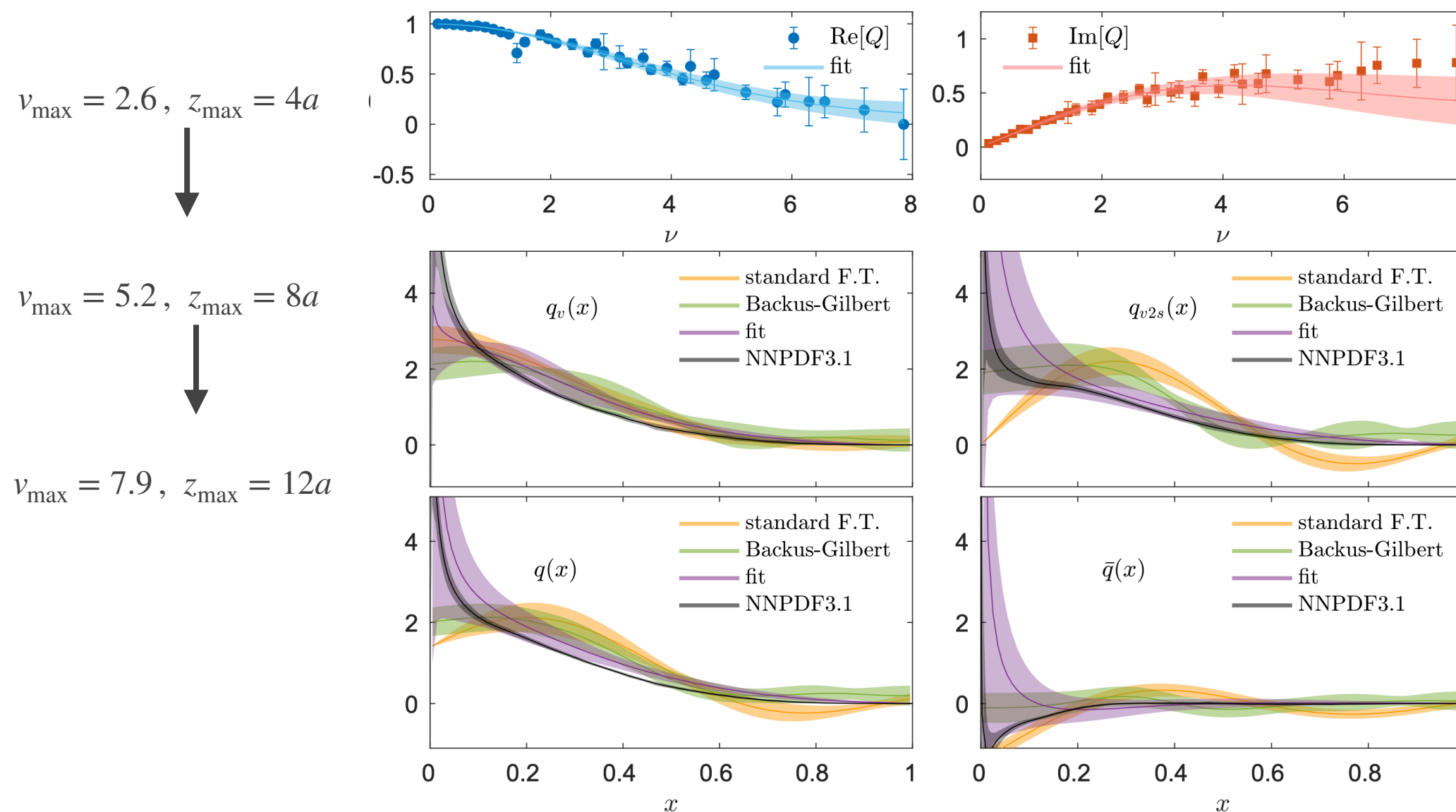
$v_{\max} = 2.6, z_{\max} = 4a$



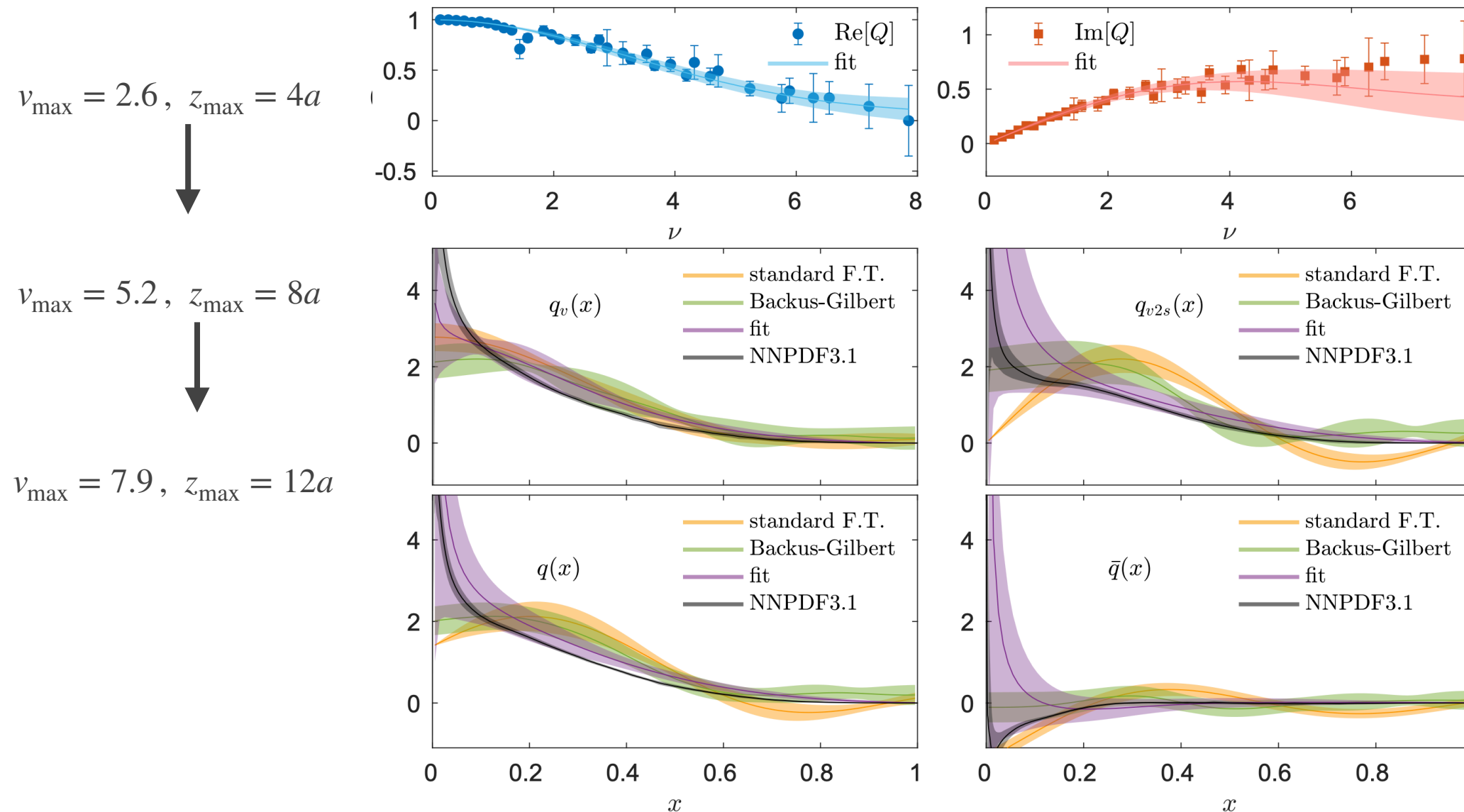
Comparison of reconstruction methods



Comparison of reconstruction methods



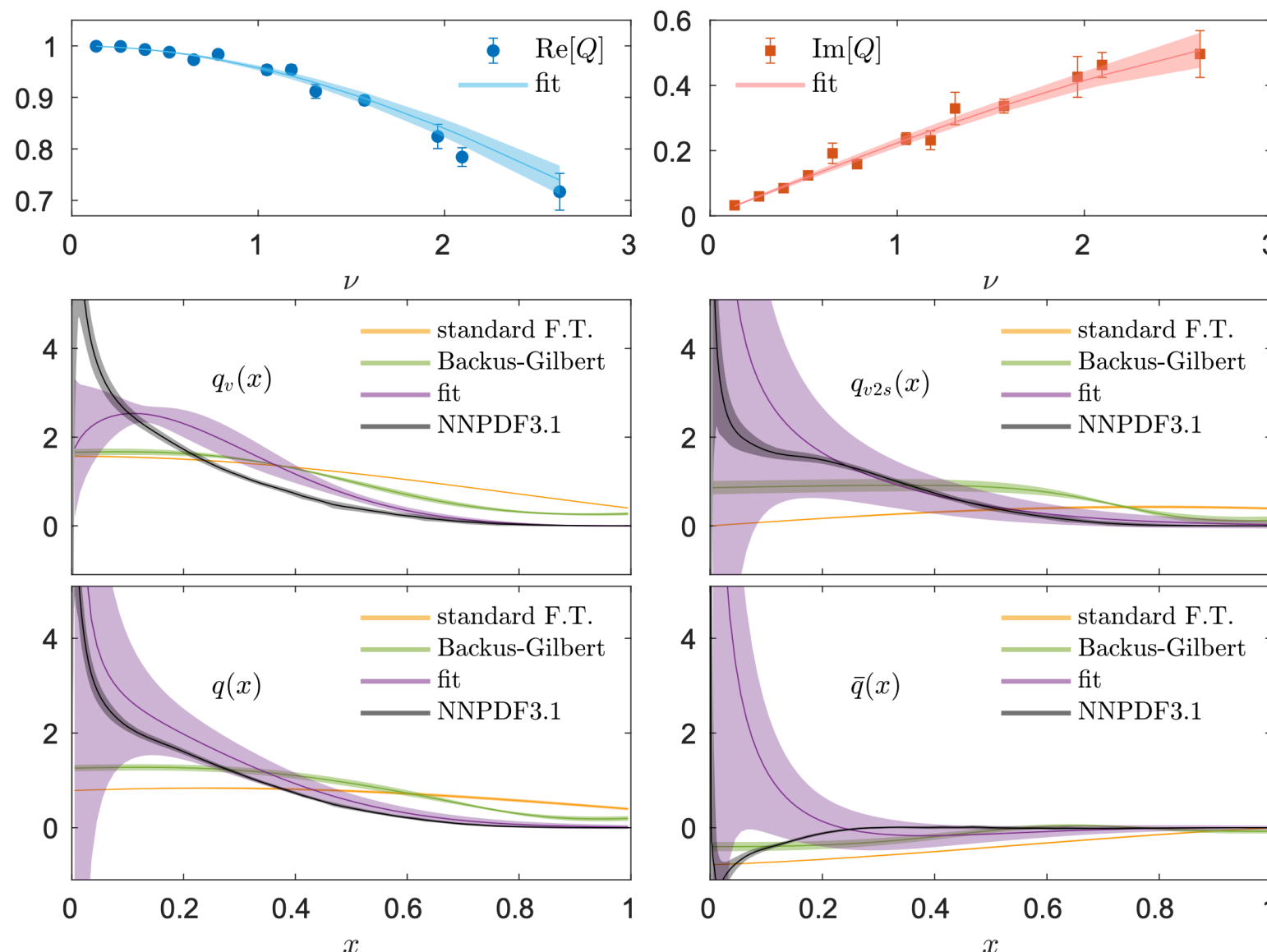
Comparison of reconstruction methods



- ★ Shape of standard FT approaches phenom. data as ν increases.
However oscillatory behavior increases. Errors do not reflect lack of data

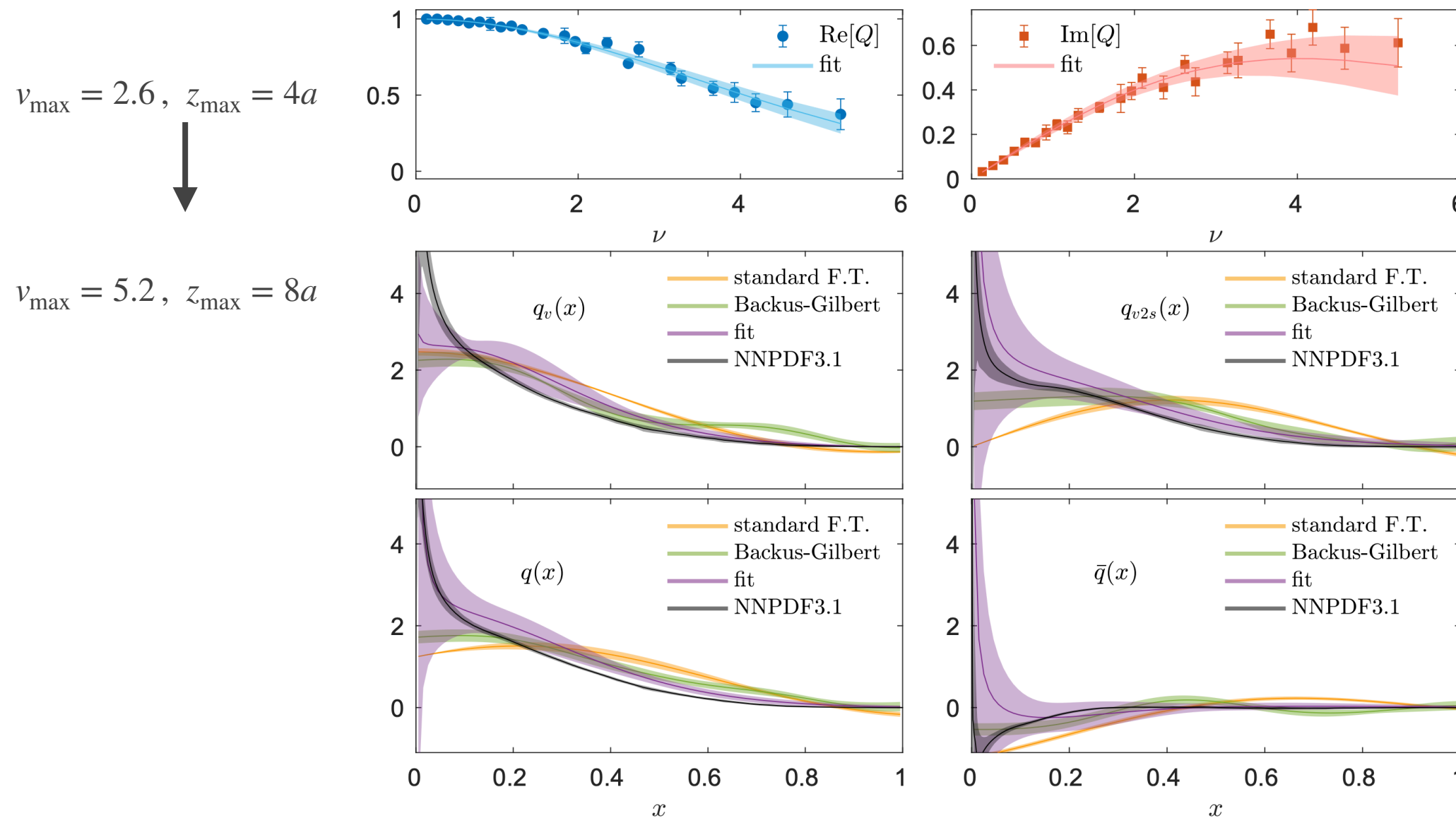
Comparison of reconstruction methods

$v_{\max} = 2.6, z_{\max} = 4a$



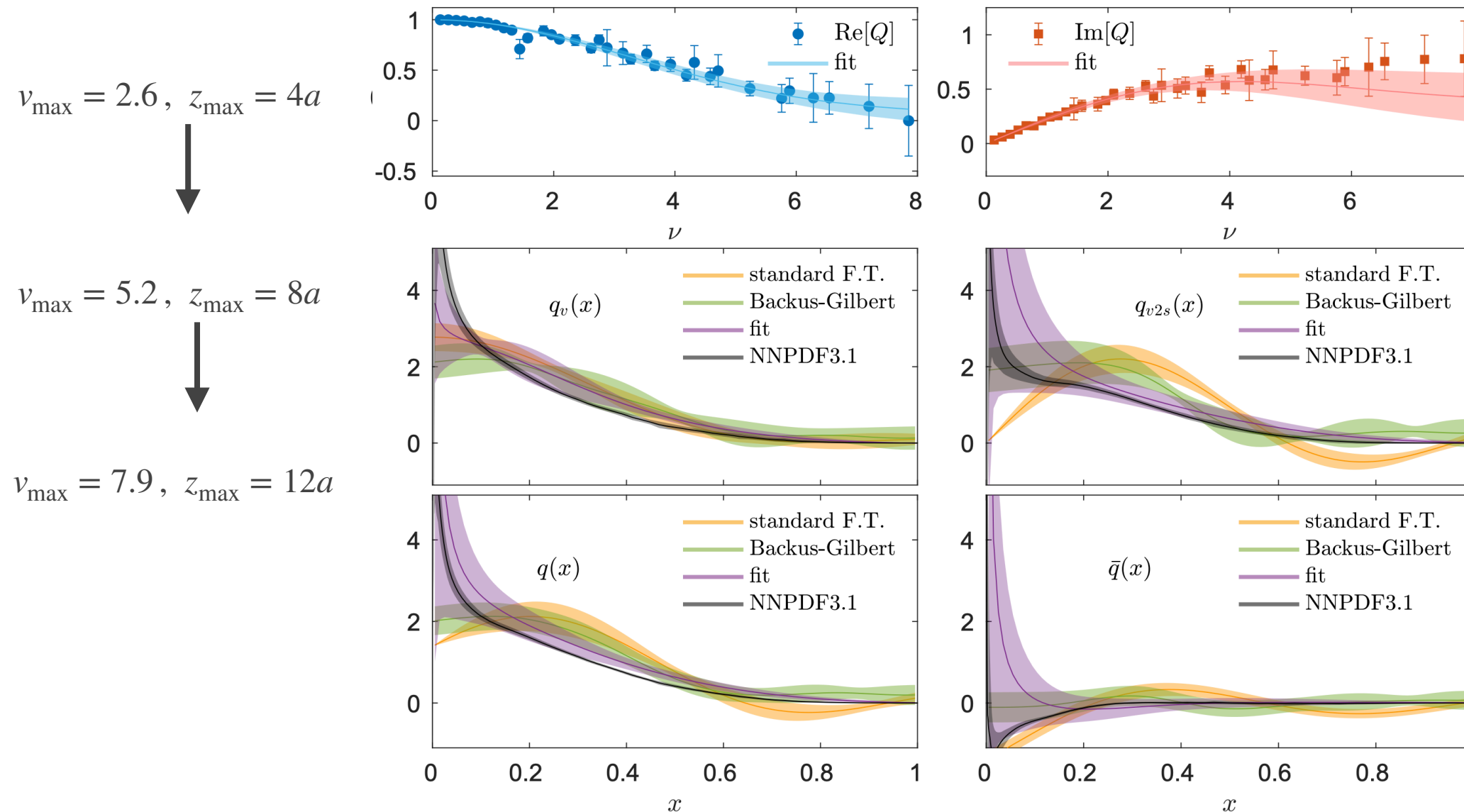
- ★ Shape of standard FT approaches phenom. data as ν increases.
However oscillatory behavior increases. Errors do not reflect lack of data

Comparison of reconstruction methods



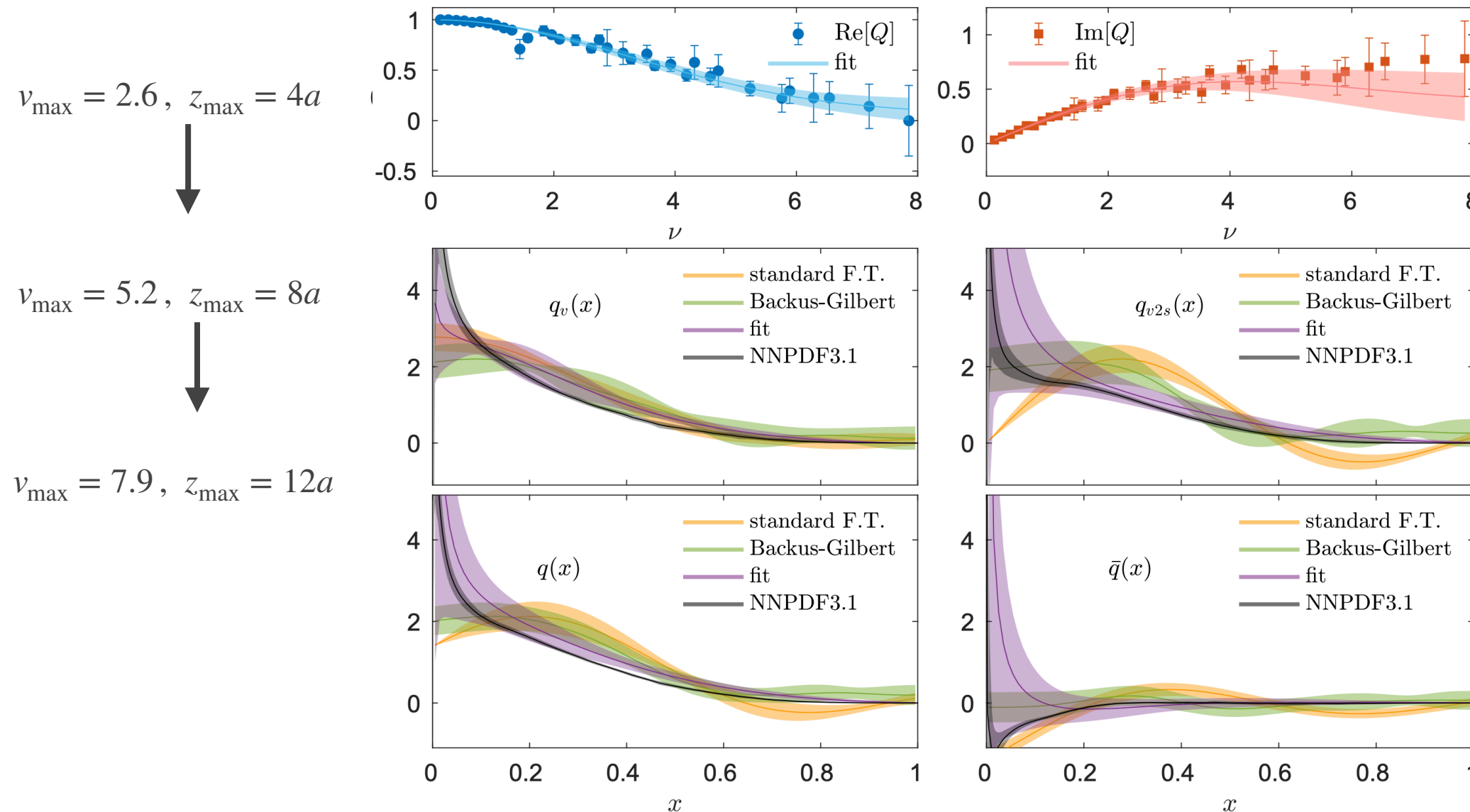
- ★ Shape of standard FT approaches phenom. data as ν increases.
However oscillatory behavior increases. Errors do not reflect lack of data

Comparison of reconstruction methods



- ★ Shape of standard FT approaches phenom. data as ν increases.
However oscillatory behavior increases. Errors do not reflect lack of data

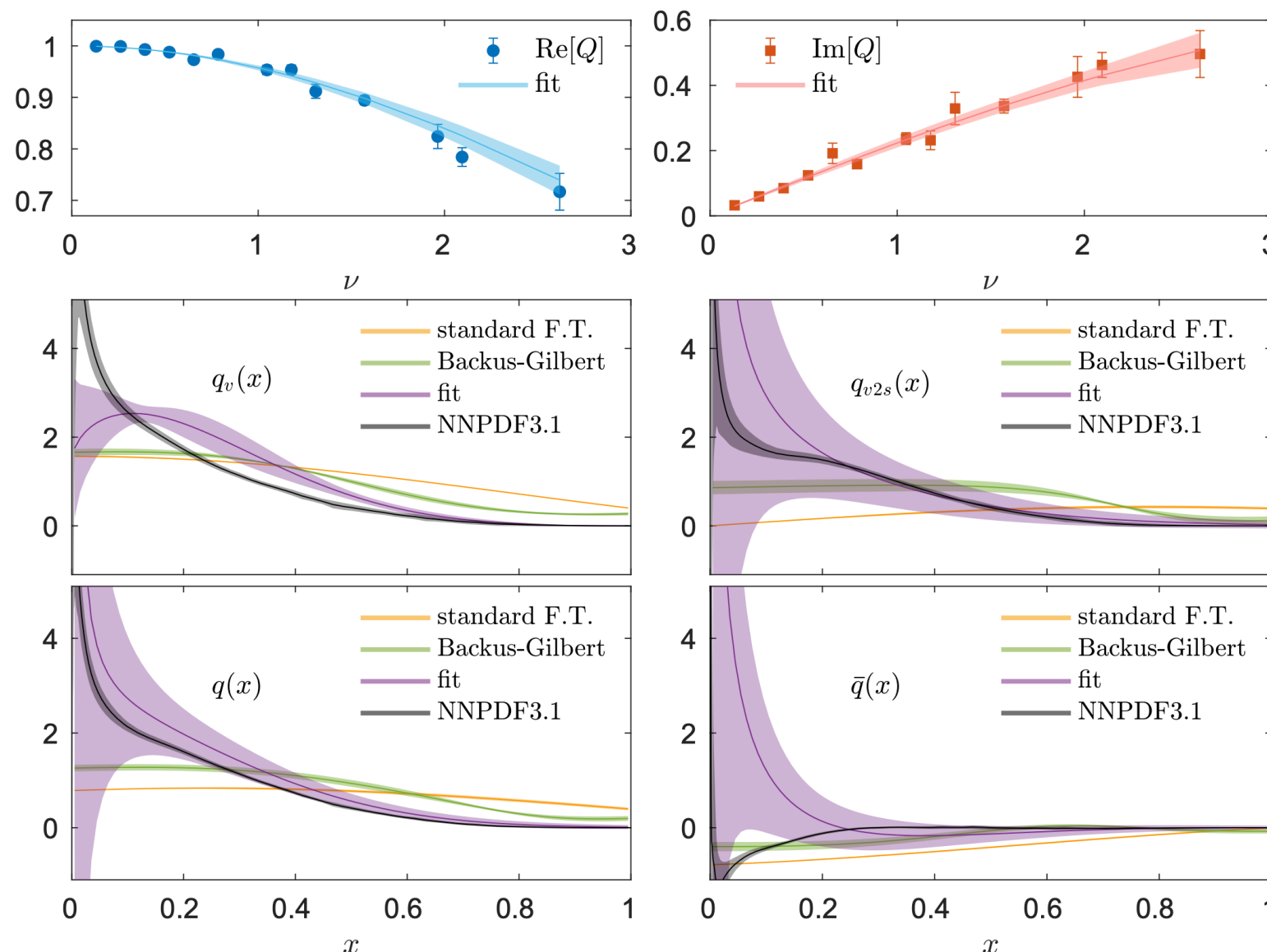
Comparison of reconstruction methods



- ★ Shape of standard FT approaches phenom. data as ν increases. However oscillatory behavior increases. Errors do not reflect lack of data
- ★ BG smaller oscillations than FT. PDF converges at about $v_{\max} = 5.2$

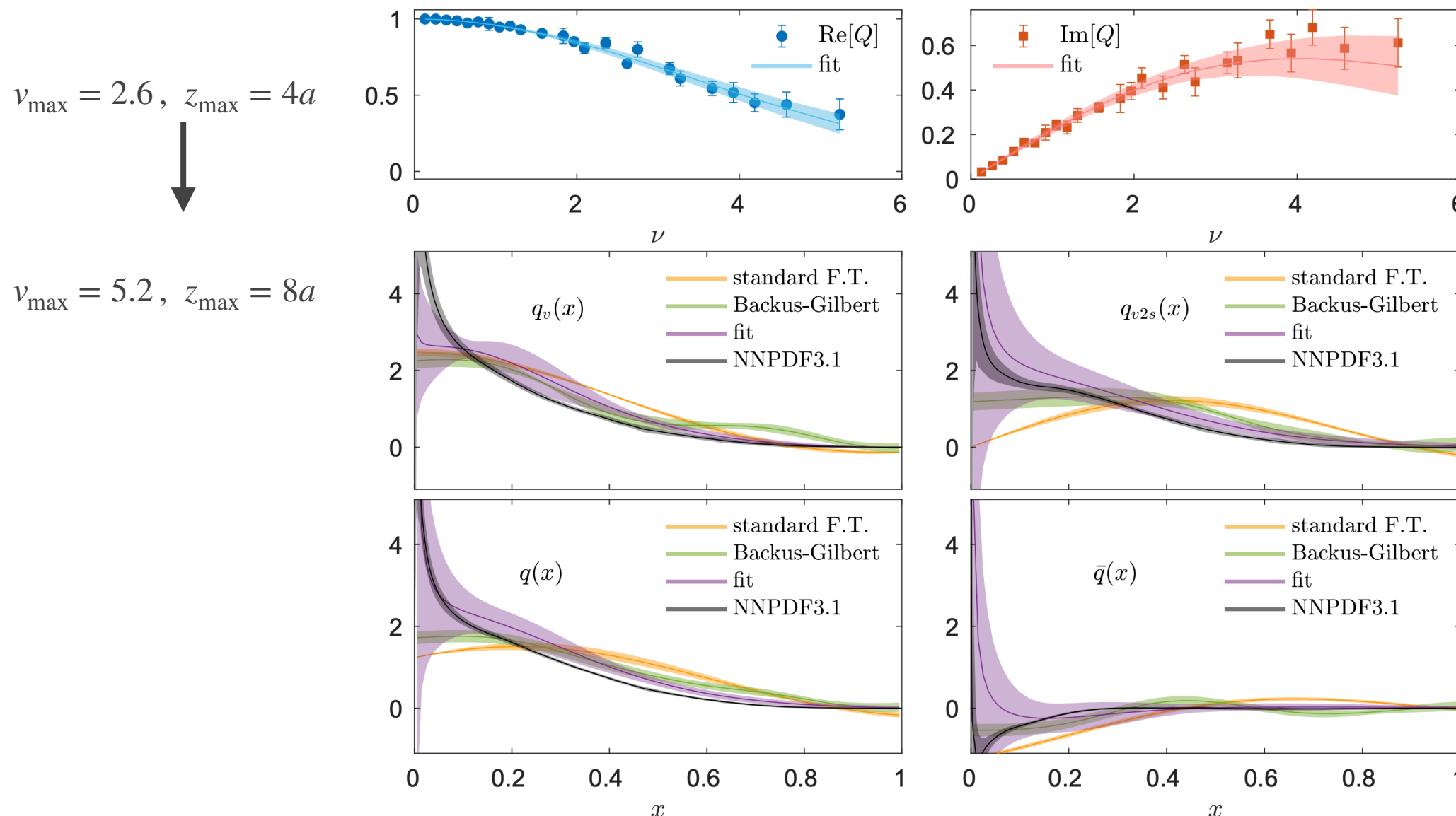
Comparison of reconstruction methods

$v_{\max} = 2.6, z_{\max} = 4a$



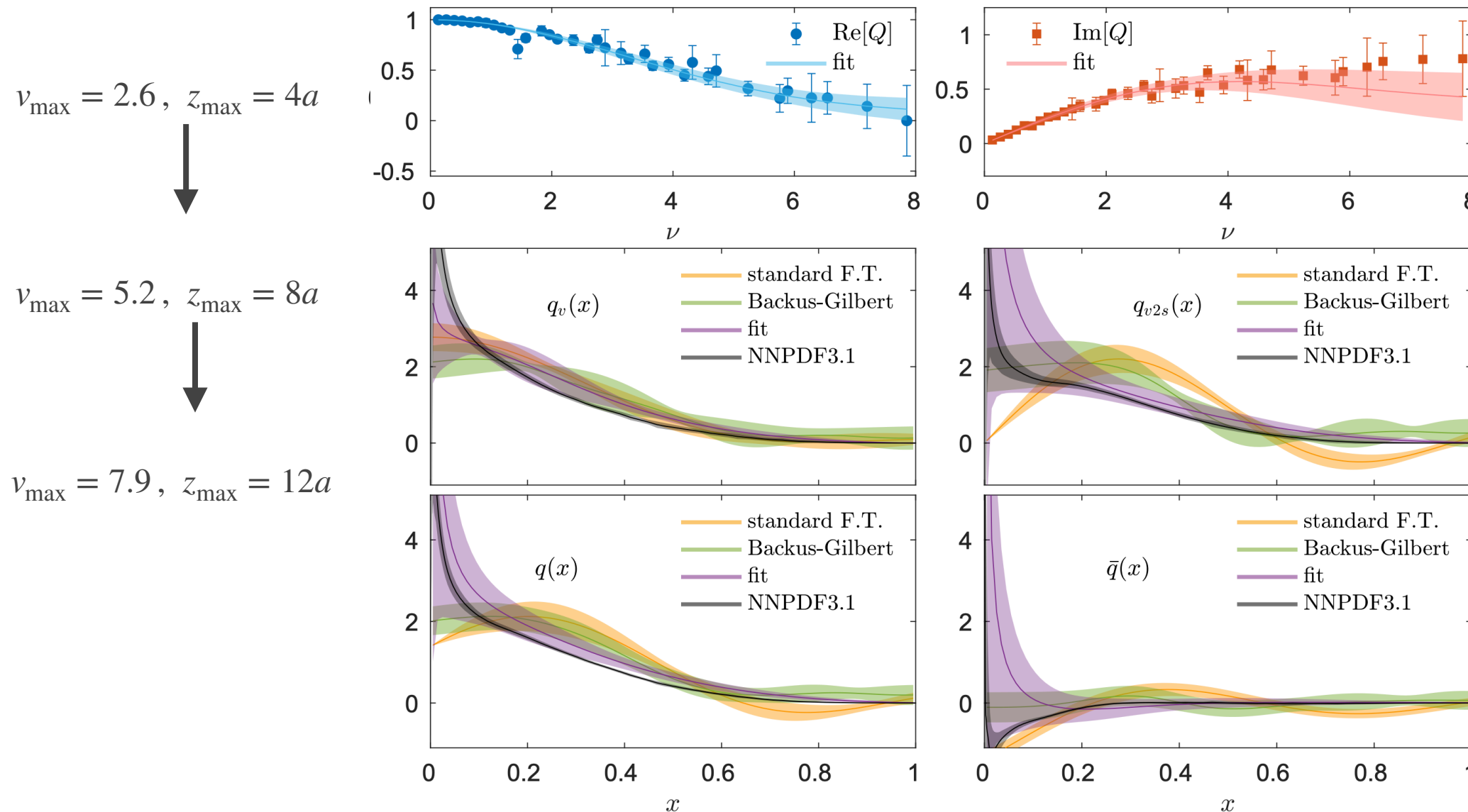
- ★ Shape of standard FT approaches phenom. data as ν increases.
However oscillatory behavior increases. Errors do not reflect lack of data
- ★ BG smaller oscillations than FT. PDF converges at about $v_{\max} = 5.2$

Comparison of reconstruction methods



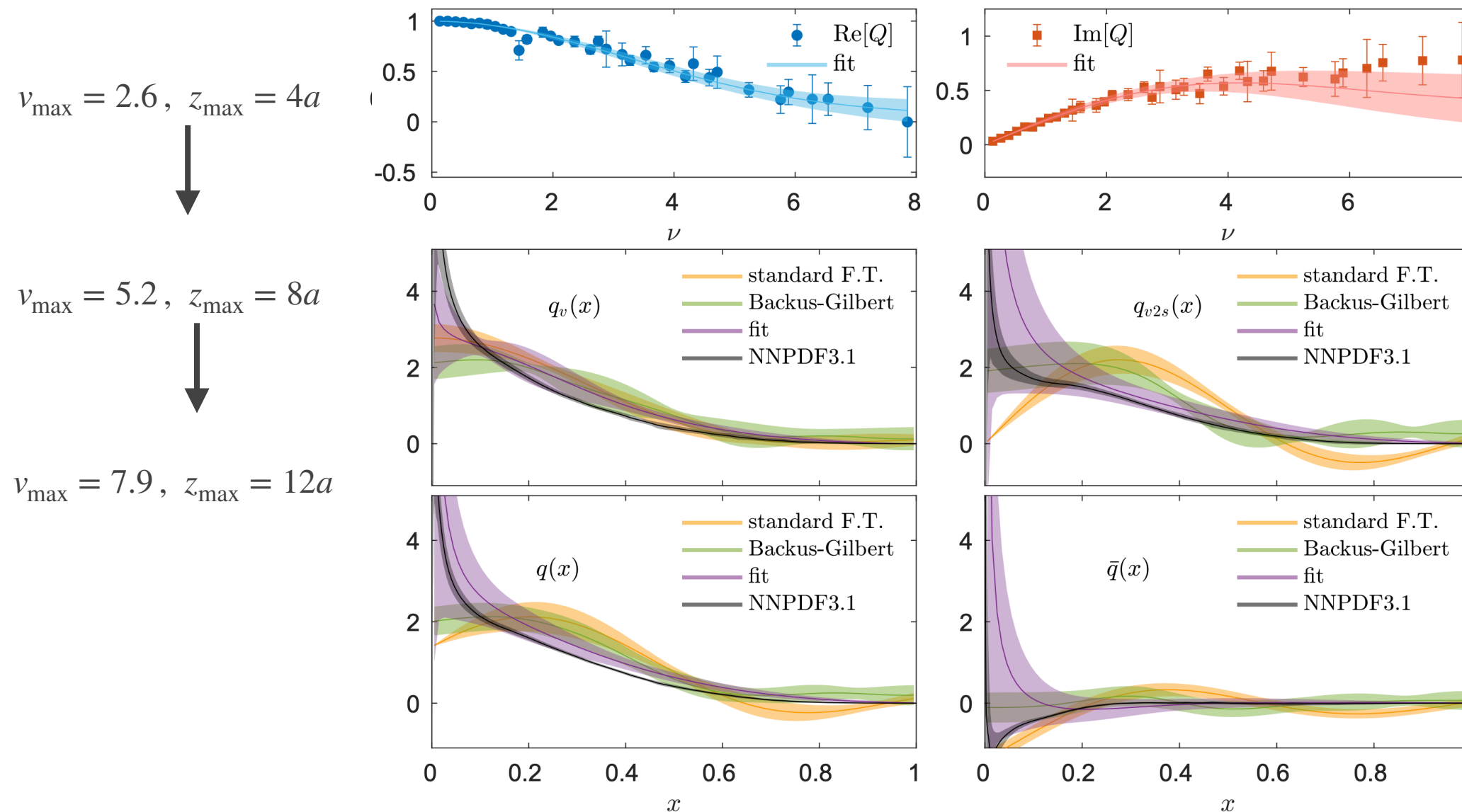
- ★ Shape of standard FT approaches phenom. data as ν increases.
However oscillatory behavior increases. Errors do not reflect lack of data
- ★ BG smaller oscillations than FT. PDF converges at about $v_{\max} = 5.2$

Comparison of reconstruction methods



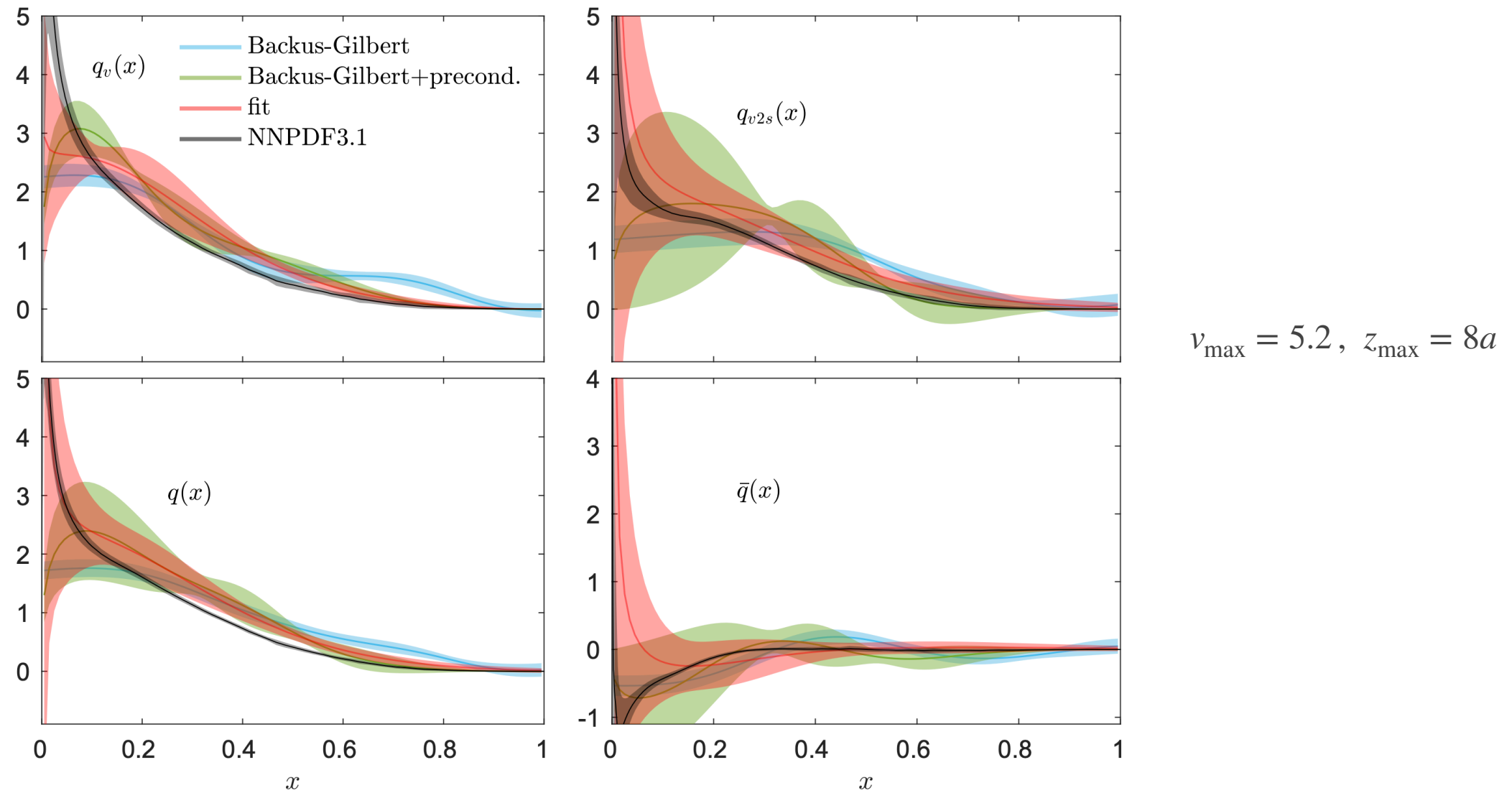
- ★ Shape of standard FT approaches phenom. data as ν increases.
However oscillatory behavior increases. Errors do not reflect lack of data
- ★ BG smaller oscillations than FT. PDF converges at about $v_{\max} = 5.2$

Comparison of reconstruction methods



- ★ Shape of standard FT approaches phenom. data as ν increases.
However oscillatory behavior increases. Errors do not reflect lack of data
- ★ BG smaller oscillations than FT. PDF converges at about $v_{\max} = 5.2$
- ★ Smooth behavior for all v_{\max} values, and compatible with phenom. data

Comparison of reconstruction methods

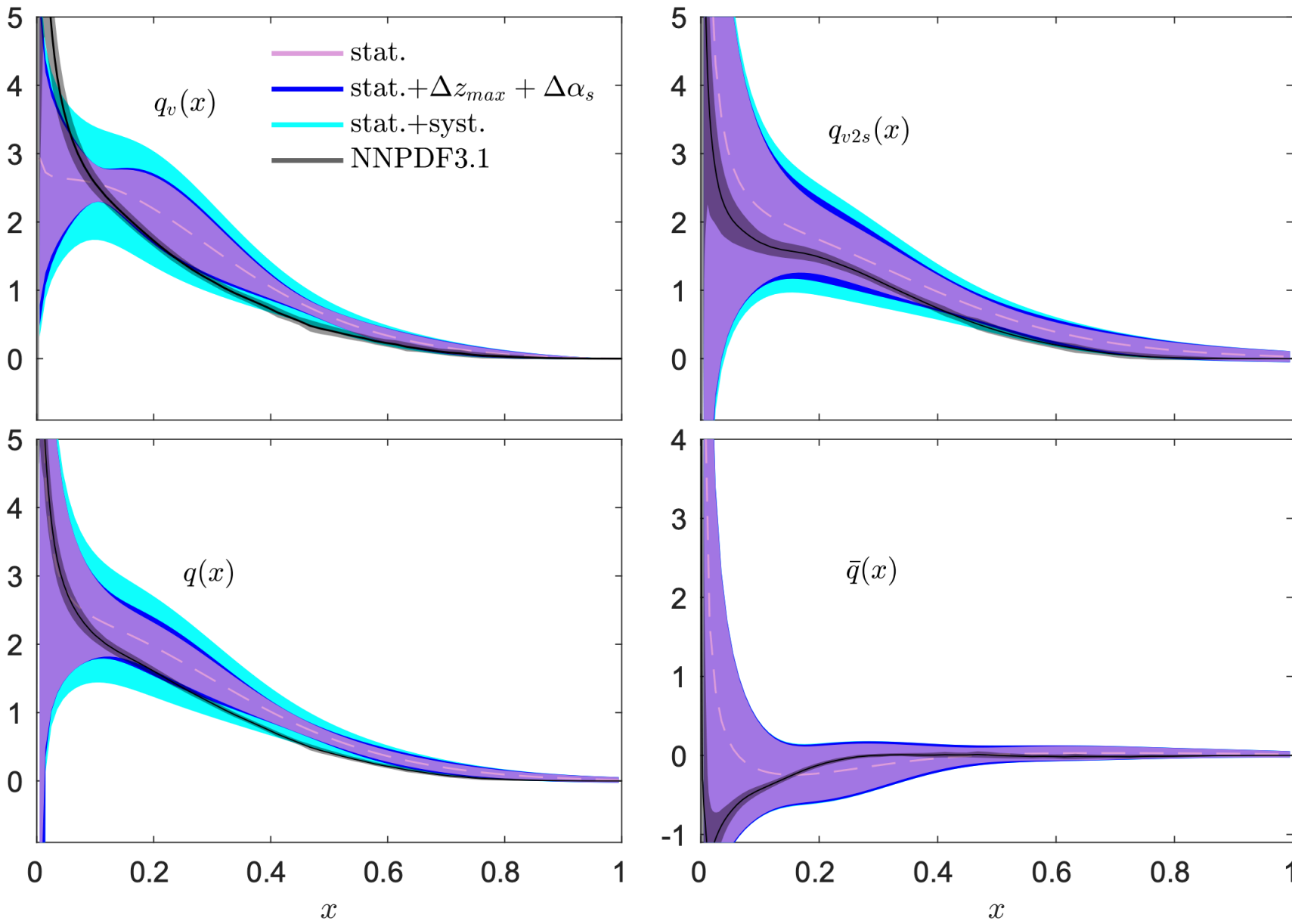


[M. Bhat et al. (ETMC) PRD 103 (2021) 3, 034510, arXiv:2005.02102]

- ★ Preconditioning in BG improves reconstruction
- ★ Fitting reconstruction performs better than BG
- ★ Conclusions hold for specific input data

Final lattice data

- ★ Exploration of systematic uncertainties and various reconstruction methods leads to a better understanding in the comparison with global analyses of experimental data

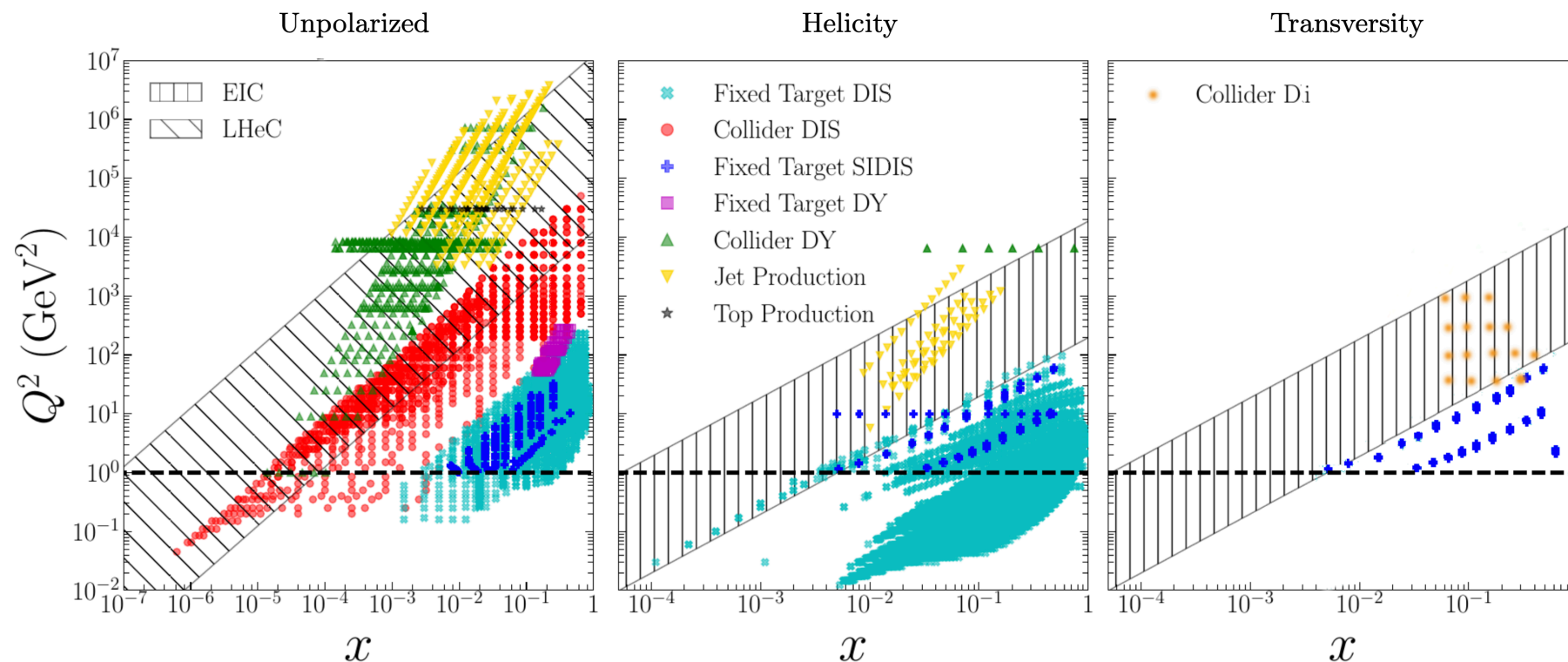


[M. Bhat et al. (ETMC) PRD 103 (2021) 3, 034510, arXiv:2005.02102]

Synergy between lattice and phenomenology

Incorporating lattice PDFs in global analyses

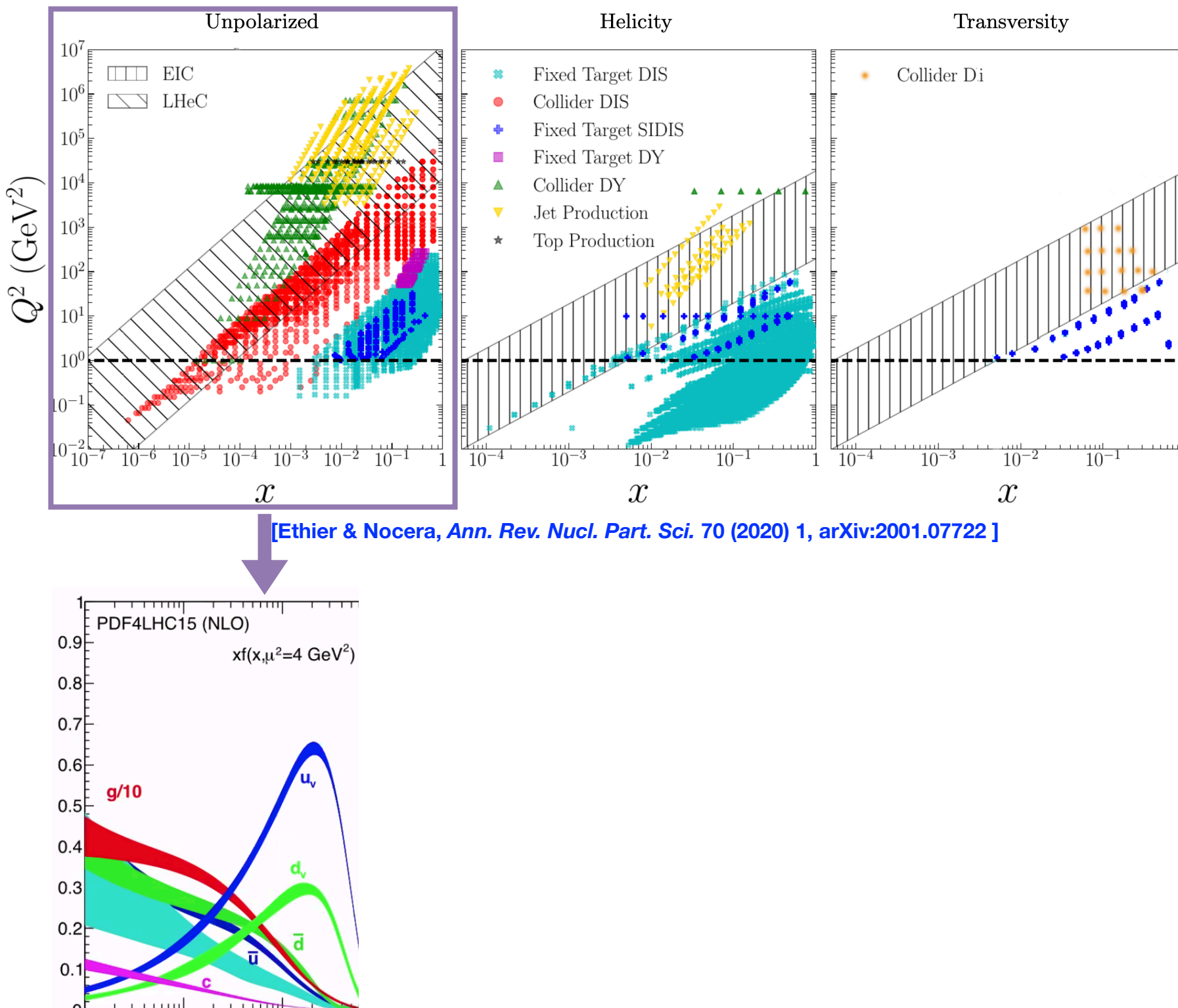
Can PDFs be better constrained in regions where experimental data are sparse, imprecise, or non-existing?



[Ethier & Nocera, *Ann. Rev. Nucl. Part. Sci.* 70 (2020) 1, arXiv:2001.07722]

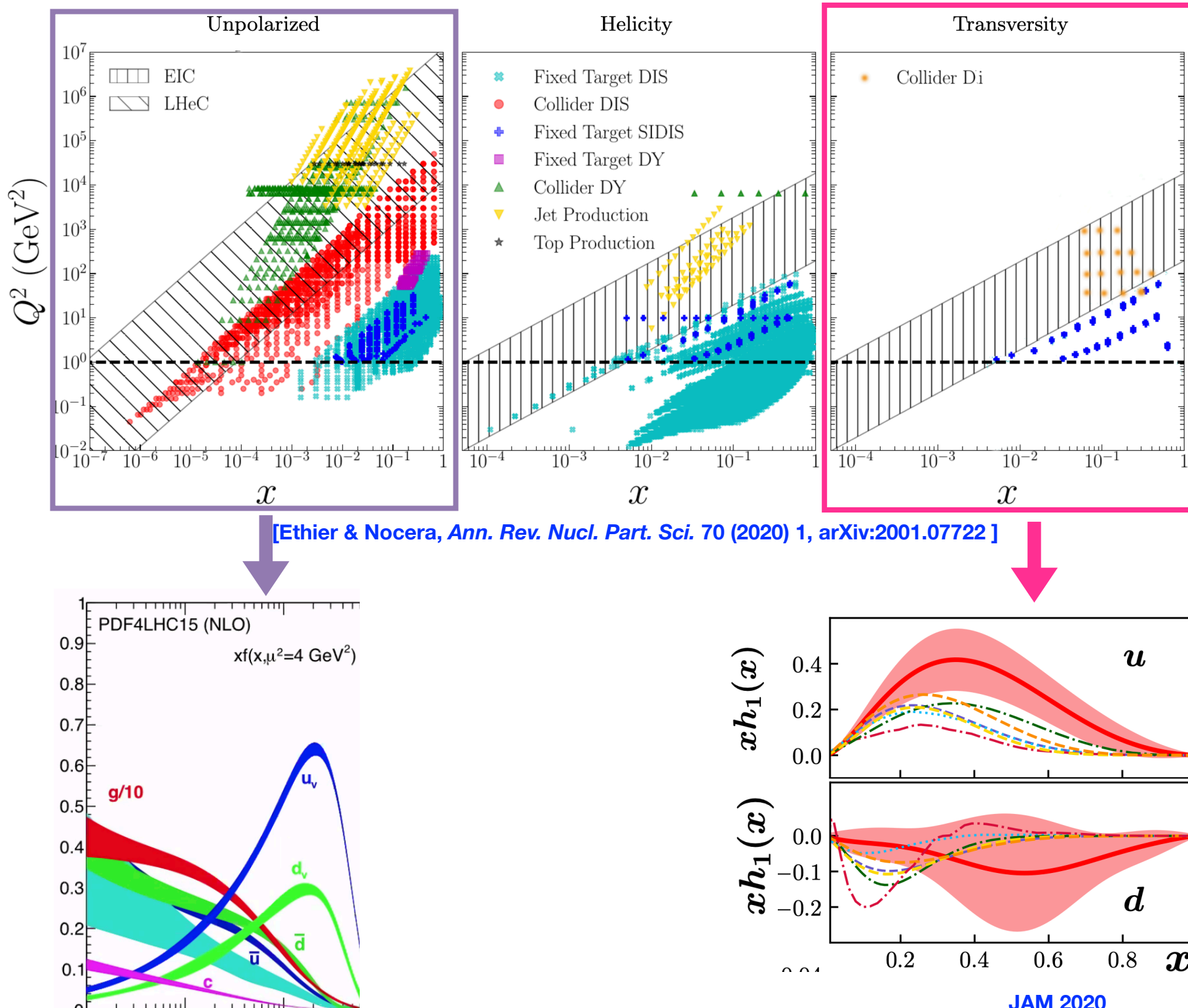
Incorporating lattice PDFs in global analyses

Can PDFs be better constrained in regions where experimental data are sparse, imprecise, or non-existing?



Incorporating lattice PDFs in global analyses

Can PDFs be better constrained in regions where experimental data are sparse, imprecise, or non-existing?



Incorporating lattice PDFs in global analyses

Synergy between lattice and phenomenology

- ★ Lattice and experimental data sets data within the same global analysis
(JAM framework)

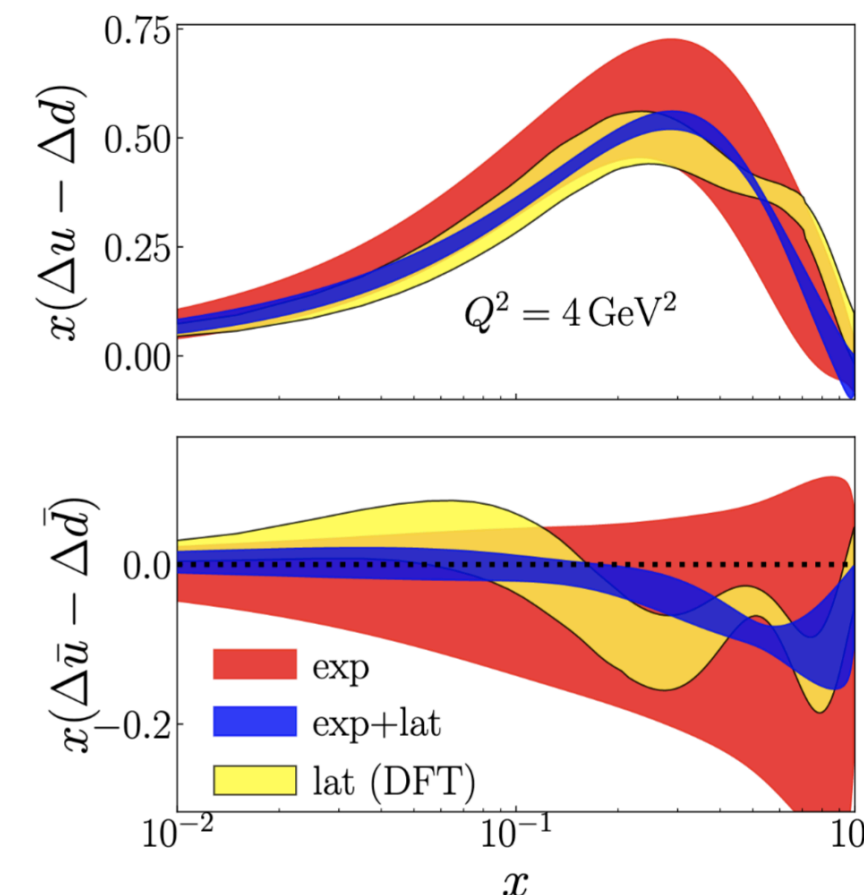
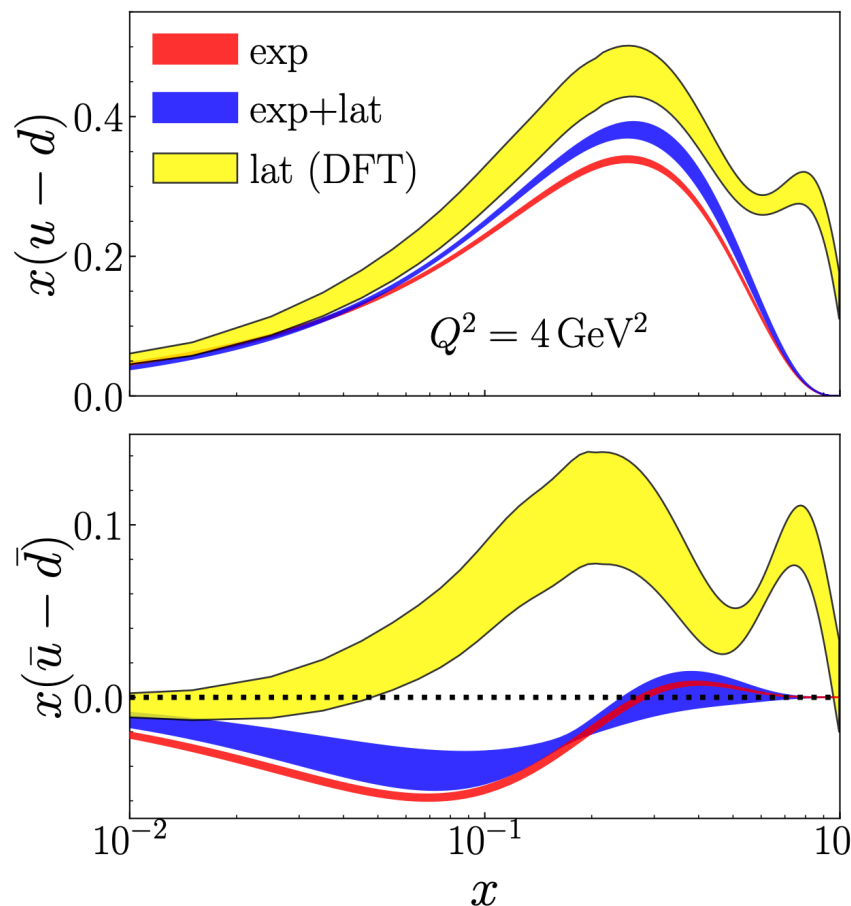
[J. Bringewatt et al., PRD 103 (2021) 016003, arXiv:2010.00548]

Incorporating lattice PDFs in global analyses

Synergy between lattice and phenomenology

- ★ Lattice and experimental data sets data within the same global analysis (JAM framework)

[J. Bringewatt et al., PRD 103 (2021) 016003, arXiv:2010.00548]



- Consistent picture with JAM for unpolarized PDF

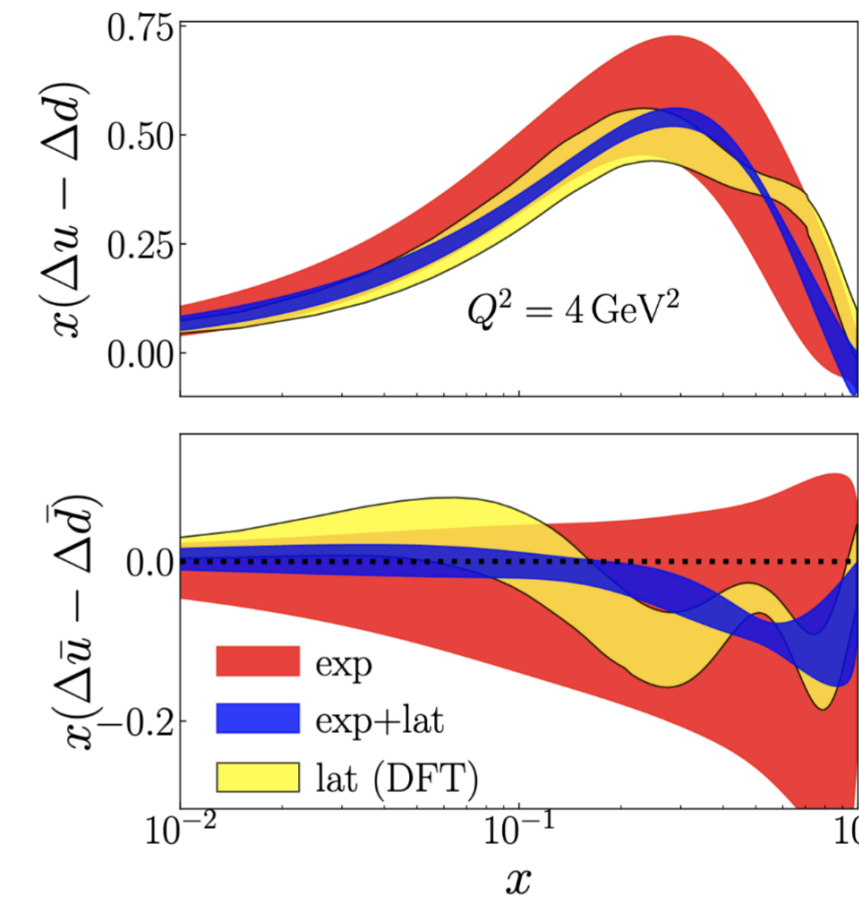
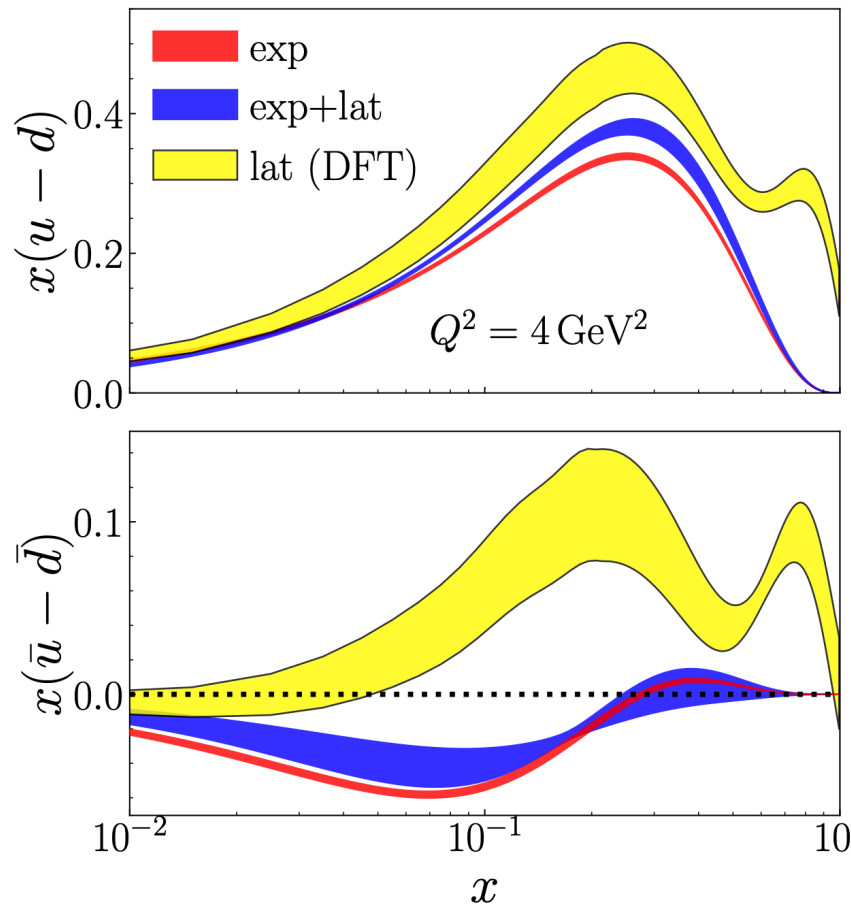
- Significant impact for helicity PDF

Incorporating lattice PDFs in global analyses

Synergy between lattice and phenomenology

- ★ Lattice and experimental data sets data within the same global analysis (JAM framework)

[J. Bringewatt et al., PRD 103 (2021) 016003, arXiv:2010.00548]



- Consistent picture with JAM for unpolarized PDF
- Significant impact for helicity PDF

- ★ Other efforts within NNPDF framework

[K. Cichy et al., JHEP 10 (2019) 137, arXiv:1907.06037]

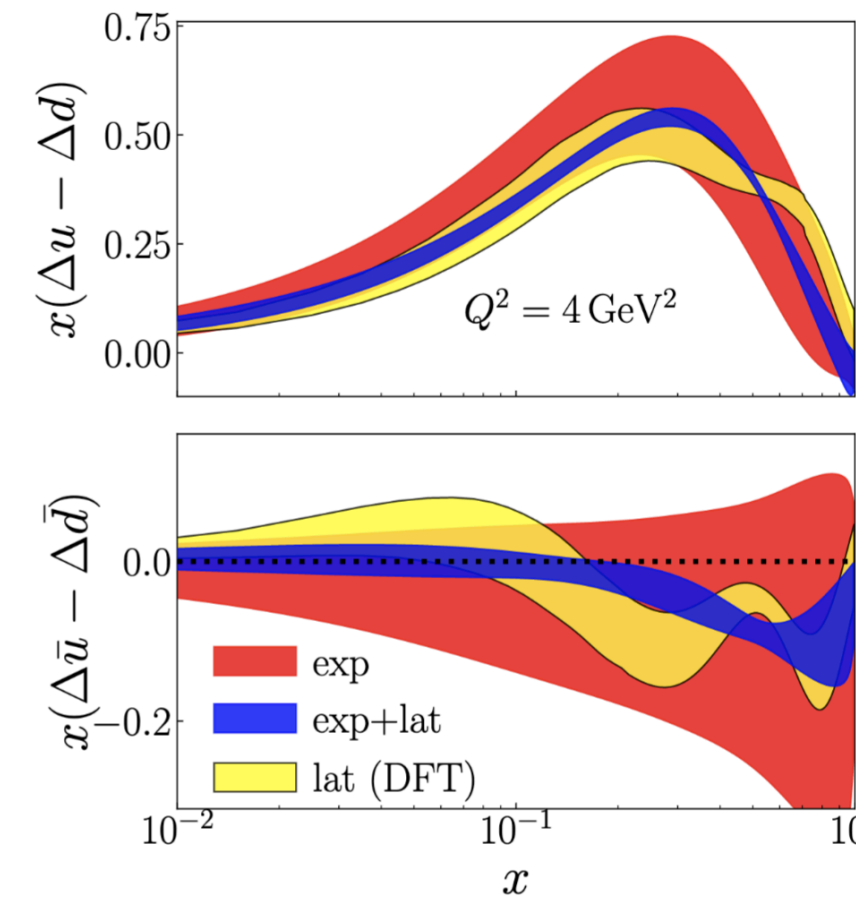
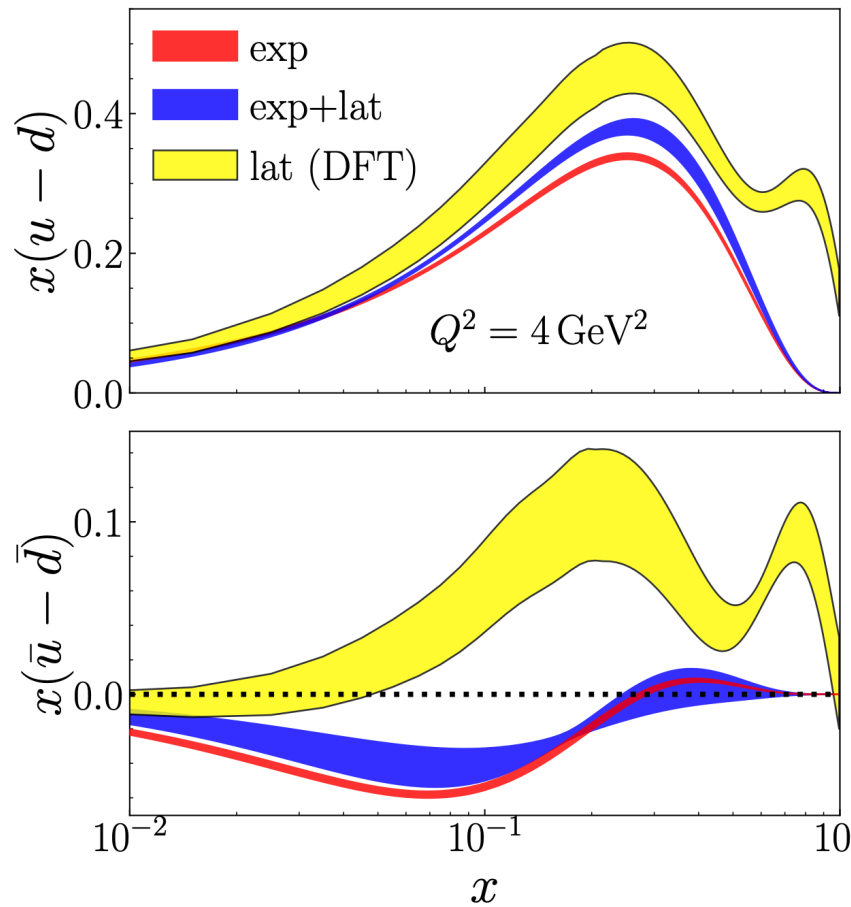
[L. Del Debbio et al., JHEP 02 (2021) 138, 2010.03996]

Incorporating lattice PDFs in global analyses

Synergy between lattice and phenomenology

- ★ Lattice and experimental data sets data within the same global analysis (JAM framework)

[J. Bringewatt et al., PRD 103 (2021) 016003, arXiv:2010.00548]



- Consistent picture with JAM for unpolarized PDF

- Significant impact for helicity PDF

- ★ Other efforts within NNPDF framework

[K. Cichy et al., JHEP 10 (2019) 137, arXiv:1907.06037]

[L. Del Debbio et al., JHEP 02 (2021) 138, 2010.03996]

- ★ Interest in applying similar approach to quantities that are more challenging to extract experimentally (GPDs, twist-3 distributions, ...)

Let's recapitulate

Concluding Remarks

- ★ **x-dependence reconstruction: Inverse problem**

[J. Karpie et al., JHEP 04 (2019) 057, arXiv:1901.05408]

Concluding Remarks

★ x-dependence reconstruction: Inverse problem

[J. Karpie et al., JHEP 04 (2019) 057, arXiv:1901.05408]

- ◆ Standard Fourier transform ill-defined

$$\tilde{q}(x, P_3) = \frac{2P_3}{4\pi} \sum_{z=-z_{\max}}^{z_{\max}} e^{-ixP_3 z} h_\Gamma(P_3, z)$$

- ◆ Derivative method problematic

$$\tilde{q}(x) = h(z) \frac{e^{ixzP_3}}{2\pi ix} \Big|_{-z_{\max}}^{z_{\max}} - \int_{-z_{\max}}^{z_{\max}} \frac{dz}{2\pi} \frac{e^{ixzP_3}}{ix} h'(z)$$

Concluding Remarks

★ **x-dependence reconstruction: Inverse problem**

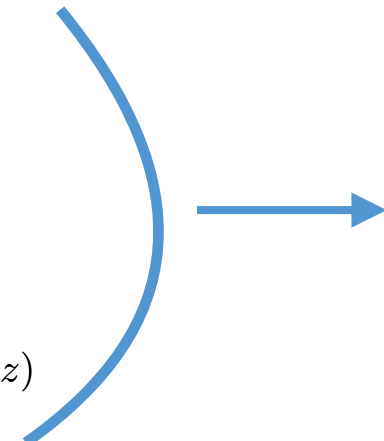
[J. Karpie et al., JHEP 04 (2019) 057, arXiv:1901.05408]

- ◆ Standard Fourier transform ill-defined

$$\tilde{q}(x, P_3) = \frac{2P_3}{4\pi} \sum_{z=-z_{\max}}^{z_{\max}} e^{-ixP_3 z} h_\Gamma(P_3, z)$$

- ◆ Derivative method problematic

$$\tilde{q}(x) = h(z) \frac{e^{ixzP_3}}{2\pi ix} \Big|_{-z_{\max}}^{z_{\max}} - \int_{-z_{\max}}^{z_{\max}} \frac{dz}{2\pi} \frac{e^{ixzP_3}}{ix} h'(z)$$



Rely on assumptions
that introduce bias in
the reconstruction

Concluding Remarks

★ **x-dependence reconstruction: Inverse problem**

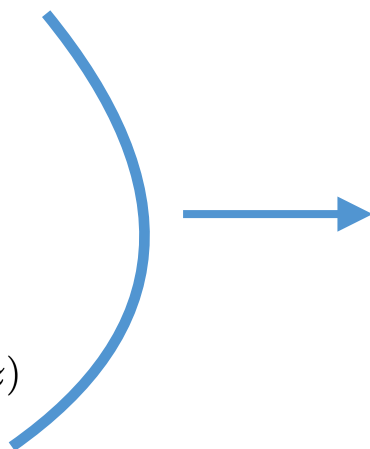
[J. Karpie et al., JHEP 04 (2019) 057, arXiv:1901.05408]

- ◆ Standard Fourier transform ill-defined

$$\tilde{q}(x, P_3) = \frac{2P_3}{4\pi} \sum_{z=-z_{\max}}^{z_{\max}} e^{-ixP_3 z} h_\Gamma(P_3, z)$$

- ◆ Derivative method problematic

$$\tilde{q}(x) = h(z) \frac{e^{ixzP_3}}{2\pi ix} \Big|_{-z_{\max}}^{z_{\max}} - \int_{-z_{\max}}^{z_{\max}} \frac{dz}{2\pi} \frac{e^{ixzP_3}}{ix} h'(z)$$



Rely on assumptions
that introduce bias in
the reconstruction

Advanced PDF reconstructions

- ◆ Backus-Gilbert Method
- ◆ Neural Network Reconstruction
- ◆ Bayesian PDF reconstruction
- ◆ Bayes-Gauss-Fourier transform

Concluding Remarks

★ **x-dependence reconstruction: Inverse problem**

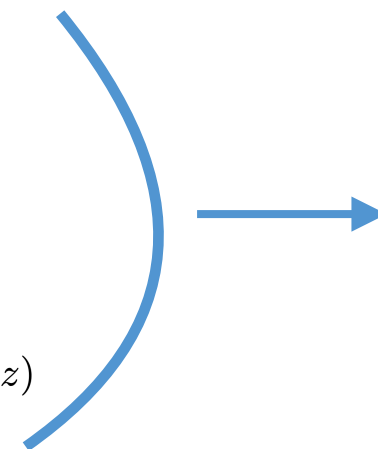
[J. Karpie et al., JHEP 04 (2019) 057, arXiv:1901.05408]

- ◆ Standard Fourier transform ill-defined

$$\tilde{q}(x, P_3) = \frac{2P_3}{4\pi} \sum_{z=-z_{\max}}^{z_{\max}} e^{-ixP_3 z} h_\Gamma(P_3, z)$$

- ◆ Derivative method problematic

$$\tilde{q}(x) = h(z) \frac{e^{ixzP_3}}{2\pi ix} \Big|_{-z_{\max}}^{z_{\max}} - \int_{-z_{\max}}^{z_{\max}} \frac{dz}{2\pi} \frac{e^{ixzP_3}}{ix} h'(z)$$



Rely on assumptions
that introduce bias in
the reconstruction

Advanced PDF reconstructions

- ◆ Backus-Gilbert Method
- ◆ Neural Network Reconstruction
- ◆ Bayesian PDF reconstruction
- ◆ Bayes-Gauss-Fourier transform

★ **Negative-x region: anti-quark contribution currently suffers from enhanced uncertainties**

Concluding Remarks

★ x-dependence reconstruction: Inverse problem

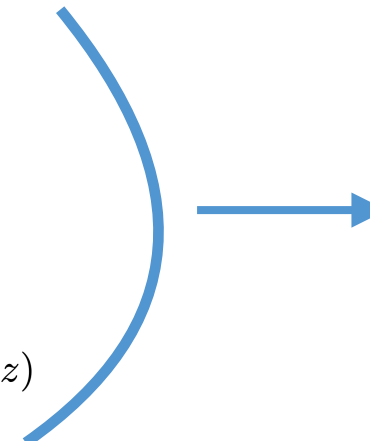
[J. Karpie et al., JHEP 04 (2019) 057, arXiv:1901.05408]

- ◆ Standard Fourier transform ill-defined

$$\tilde{q}(x, P_3) = \frac{2P_3}{4\pi} \sum_{z=-z_{\max}}^{z_{\max}} e^{-ixP_3 z} h_\Gamma(P_3, z)$$

- ◆ Derivative method problematic

$$\tilde{q}(x) = h(z) \frac{e^{ixzP_3}}{2\pi ix} \Big|_{-z_{\max}}^{z_{\max}} - \int_{-z_{\max}}^{z_{\max}} \frac{dz}{2\pi} \frac{e^{ixzP_3}}{ix} h'(z)$$



Rely on assumptions
that introduce bias in
the reconstruction

Advanced PDF reconstructions

Thank you

- ◆ Backus-Gilbert Method
- ◆ Neural Network Reconstruction
- ◆ Bayesian PDF reconstruction
- ◆ Bayes-Gauss-Fourier transform



DOE Early Career Award (NP)
Grant No. DE-SC0020405

- ★ Negative-x region: anti-quark contribution currently suffers from enhanced uncertainties



TMD Topical
Collaboration